# CHARACTERIZATION OF A FLUID FILLED COMPOSITE FOR RADIATION PROTECTION

By

LEROY GARLEY JR

Bachelor of Science in Mechanical Engineering

New Mexico Institute of Mining of Technology 2006

Socorro, New Mexico, USA

Submitted to the Faculty of the
Graduate College of the
New Mexico Institute of Mining and Technology
in partial fulfillment of
the requirements for
the Degree of
MASTER OF SCIENCE
January 23, 2015

CHARACTERIZATION OF A FLUID FILLED

COMPOSITE FOR RADIATION PROTECTION

Independent Study Approved:

Dr. Ashok Kumar Ghosh

---

Study Adviser

Dr. Warren Ostergren

---

Committee Member

Dr. Arup Maji

---

Committee Member

Name: LEROY GARLEY JR

Date of Degree: January 23, 2015

Title of Study: CHARACTERIZATION OF A FLUID FILLED COMPOSITE FOR RADIATION PROTECTION

Major Field: MECHANICAL ENGINEERING

Abstract:

A fluid filled composite material has been created for radiation shielding based upon a material that was previously tested for noise suppression and structural applications. The three main focus areas of the work were to analyze materials and finalize the test material based on the fluid filled composite patent (US7,947,364 B2) received by NMT on May 24, 2011

This study was completed to help solve the problem of radiation exposure to humans working with radioactive materials, those traveling in space as well as those affected by nuclear accidents. Specifically, the aim was to develop a durable lightweight material that could shield humans and other radiation sensitive objects while reducing weight of standard shielding materials usually made of Lead (Pb).

Different composite materials were created based on the fluid filled composite previously mentioned. Additional materials were added in different processes to induce certain specific properties. Once a material was deemed to be sufficiently mature it was analyzed in the computer simulation tool SRIM-Stopping & Ranging of Ions in Matter.

The SRIM results show that different interstitial compounds were able to magnify the energy absorption properties of the base material. The overall positive trend was then compared to the lead shielding. While the material did not perform to the level of the lead for a given thickness, the material could be made thicker to achieve the same total stopping power while still reducing overall weight.

Once the final group of materials was selected, samples were made for exposure testing. The materials were exposed to differing levels of Gamma radiation from a Cobalt-60 source. Post radiation testing was conducted to see the reduction in strength of the composites face and rear layer. As expected, the front face had a much higher reduction in strength compared to the rear face in almost every case except for the control samples.

# Table of Contents

# LIST OF FIGURES

CHAPTER I

BACKGROUND INFORMATION

# 1. Background Information

## 1.1. Types of Ionizing Radiation

There are four main types of Ionizing radiation that will be encountered while protecting from nuclear radiation. These are the alpha particle (α), the Beta particle (β), the Gamma ray (γ) and the neutron (n).

The Alpha particle is essentially a Helium nucleus with a 2+ charge ($He^{2+}$) consisting of two protons and 2 neutrons. This particle is created by a process called alpha decay and is most notably part of the decomposition of uranium into thorium. Alpha particles can be created by other means but are usually only created by the decomposition of elements greater than 83 atomic weight units [1]. Alpha particles are considered to be the most dangerous to humans if they are in direct contact with the skin or are ingested by breathing or swallowing. The particle can cause severe DNA mutation and chromosome damage. This damage is in a relatively close area to the particle only; most approximations are listed at ½ inch or less [1]. However, as powerful as this particle is, it can be stopped with just one sheet of notebook paper or similar thin barrier. This makes it very easy to protect humans from alpha radiation poisoning.

The Beta particle is a high speed electron or positron emitted by a process called beta decay. In the case of nuclear reactions generally only the electron form of the Beta particle is emitted. This happens by conversion of a neutron into a proton, electron and an antineutrino [1]. The process is common in neutron rich environments; however, the complex physics is

beyond the scope of this project. Unlike the alpha particle, the Beta can be created by atoms of less than 83 atomic mass units. It generally has a medium level of energy compared to the alpha and gamma ray; however, each beta particle has a varying level of energy depending on the parent atom. To protect from beta particles only a thin sheet of low density plastic or aluminum is needed; the particle will slow down and eventually stop inside the metal by electromagnetic means.

Third on the list is the Gamma ray, unlike the alpha and beta particles, the gamma ray has no physical mass; it is electromagnetic radiation of very high frequency [1]. Gamma rays can be created by many means; one commonly encountered is due to gamma decay. This is the decay of high energy states in atomic nuclei. Another creation method is nuclear fission where an atom is split and releases energy, free neutrons, and gamma rays. The gamma ray, like the alpha and beta can cause extensive damage; however, it disperses its energy over a much larger area so the local effects are not as great. The damage caused by gamma rays is almost always internal and is the greatest cause of radiation sicknesses since it is so hard to protect from. The gamma ray is generally shielded by using atoms with large atomic mass. There are many materials used to accomplish this; the most common is lead which is mainly used due to its availability and its dense structure. One misconception is that a metal must be used, but research shows that many aggregate products such as granite and concrete do an equally good job shielding with sufficient thickness [2]. The main goal is to put as much mass between the individual and the gamma ray emitter. Figure 1 is taken from the US Air Force Survival Manual and lists common materials and the thickness they require to reduce gamma emissions by 50%. This is known as the Halving-distance; and while not listed in the table, the halving-distance for lead is 0.5 inches.

| | |
|---|---|
| Iron and steel | .7 inches |
| Concrete | 2.2 inches |
| Brick | 2.0 inches |
| Dirt | 3.3 inches |
| Ice | 6.8 inches |
| Wood (soft) | 8.8 inches |
| Snow | 20.3 inches |

Figure 1: Common materials with the thickness required to shield gamma radiation by 50%. From US Air force Survival Handbook

The final type of particle looked at is the neutron. During the fission of Uranium 235 free neutrons are absorbed and create a momentary new $U_{236}$ atom which becomes unstable and splits into two smaller atoms and releases additional neutrons. This is a continual chain reaction where the newly released neutrons will be absorbed by another $U_{235}$ atom [3]. The rate of nuclear fission is largely controlled by the free neutrons but can be artificially altered by insertion of control rods in a nuclear reactor. Neutrons are very dangerous as they have the ability to alter molecules and atoms, but single neutrons cannot cause a chain reaction inside the human body. Unlike alpha, beta and gamma radiation the neutron cannot be affected by mass alone. Materials high with hydrogen content do a very good job of slowing down the neutrons due to complex matter interactions. Research also suggests that concrete blocks (cinderblocks) and some plastic blocks work better than metal compounds. While these materials can slow down the neutrons they must be captured. In studies, isotopes such as Lithium and Boron do a good job of capturing the excess neutrons [3].

## 1.2. Protection Fundamentals

In general, there are three fundamentals of radiation protection for war, power production and naturally occurring radiation; they are: time, distance and shielding [4].

Time- The time in an area affected by radiation is one of the easiest things to control and the less time spent in an affected area the less overall exposure received.

Distance- The distance from an emission source can only be controlled in certain situations. In the case of an operator of a nuclear reactor, they can only be as far away from emission as the work station is.

Shielding- Shielding is the ability to put absorbing or attenuating materials between the emitter and the individual. There is however no material that can completely protect from all types of radiation discussed above in an efficient way.

## 1.3. Personal Exposure Background

In the spring of 2011 I was asked to lead a team that was to travel to Japan and help with Operation Tomodachi (Operation Friendship). This was a disaster recovery effort for the people of Japan in the aftermath of the 2011 Tōhoku earthquake and tsunami. Our main mission was structural health monitoring and aerial survey of the Fukushima Dai-ichi nuclear complex. While we utilized an unmanned aerial vehicle to complete these tasks we would have to be in very close proximity to the destroyed reactors; specifically reactors 1 and 2. This is the motivation for this research project; the focus of this project is the effective shielding of workers in different radioactive loadings.

In general nuclear reactors have multiple layers of built in shielding that protect workers and contain the alpha and beta particles, contain most of the gamma rays and capture free neutrons. In these situations very little personal shielding is required for nuclear workers. The majority of those working around the reactor need nothing more than a protective jumpsuit and no respirator since the reactors have built in filtration. However, when working inside the reactor or removing spent fuel more protection is afforded to the individual. Currently the

industry standard personal protective equipment worn is a DuPont Tyvek jumpsuit, rubber gloves and boots as well as a HEPA full face respirator.

While working in the Fukushima Dai-ichi and Dai-ini compounds workers were afforded the same protective equipment as well as thick full body underwear to help stop the alpha and beta particles. The Tyvek was mainly used to reduce the possibility that the individual be exposed to chemical burns and provided an additional layer of alpha & beta particle protection. The suits were single piece and included a hood which was taped to the outside of a full face respirator for an almost airtight seal. This gave good protection from the alpha and beta particles that might be encountered at the facility but afforded no protection to the gamma rays or free neutrons. While operating the drones from a stationary point, the team I was part of was shielded from gamma rays by a 3 inch thick steel box enclosure. We were also less than 100 meters from the open end of the reactor containment vessel.

## 1.4.Historical Materials Used For Shielding

As discussed earlier there are many types of materials that can stop or slow down radiation effects. These materials have historically been dense and metallic [4]. Engineered materials designed to protect from multiple radiation types will be discussed in a later section. Lead is the frontrunner in most radiation protection situations as it can stop α, β & γ rays if it is thick enough. However it is limited in application as it is very heavy and difficult to move around; it is generally relegated to static protection or protection where maneuverability is secondary to protection such as for X-Rays in a dentist's office. Steel and Aluminum can also do a good job of dissipating radioactive energy but a greater volume is needed as they are not as dense as Lead. Concrete in slab or block form also does a very good job in static applications and can block all 4 main types of radiation with sufficient thickness [2]. Two materials that

perform in a satisfactory manner are packed earth (dirt/rock) and water. Most maneuverable materials that have been used in the past such as sheet aluminum, Tyvek and fiberglass provide good protection from α & β particle penetration and utilize distance to protect from ionizing radiation but afford little to no protection from γ rays [5].

CHAPTER II

# 2. Literature Review

## 2.1.Background

There have been many studies on single and composite materials with respect to lifespan and radiation shielding; however, there are minimal studies on fluid filled composites in radiation shielding events. The following sections will discuss radiation shielding state of the art techniques as well as past research on multi layer fluid filled composites.

## 2.2.Suitable Composites & Materials for Radiation Protection

Currently there are no thin and active shielding materials in widespread use. Only passive and bulky materials are available for radiation and magnetic protection. This restriction in the ability of the materials to be lighter and thinner will be a primary reason for stalling deeper space exploration. Materials that are lighter and more versatile will be required during future missions to deeper space including Mars [6]. Before 2002 the level of radiation exposure on a trip to mars was a guessing game with many differing opinions. The 2001 Mars Odyssey spacecraft changed that fact as it carried the Mars Radiation Environment Experiment (MARIE) which was designed to measure the radiation environment on a trip to Mars as well as during repeated orbits [7]. The experiment used a 68 degree field of view spectrometer to measure radiation in both static and dynamic events such as solar flares and cosmic bursts. The pertinent data gathered by the instrument is plotted below in Figure 2.

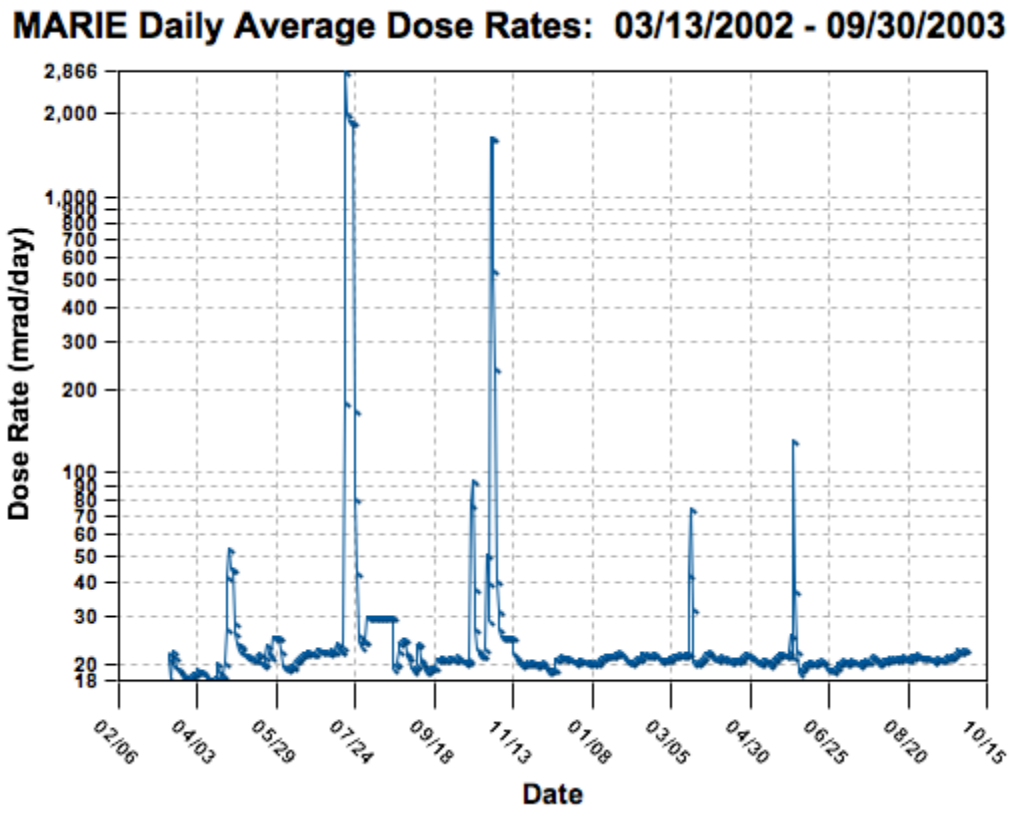


Figure 2: MARIE Dose Rates gathered on trip to Mars and in Mars orbit from [19].

The plot shows spikes where galactic events bombarded the spacecraft as well as the MARIE unit itself. According to NASA, the expected dose per year is 1.7 Gray. This number will be used to calculate a total expected dose for a round trip to Mars. Using current propulsion systems, the trip to Mars is expected to take approximately 9 months, if a team stays on the planet for 1 year the total time would be approximately 2.5 years of exposure. To calculate total dose we multiply dose rate by duration of stay.

$$Exposure = Dose\ Rate\ x\ Duration$$

$$Exposure = \frac{1.7 Gray}{year} * 2.5\ years = 4.25\ Gray$$

There is ongoing research that is showing that alternative materials are promising to increase shielding ability. One current study shows that polyethylene can be considered a frontline material with respect to radiation shielding in galactic cosmic ray environments [8]. There is dialogue that this effect is due to polyethylene having an abundance of Hydrogen atoms. This use of polyethylene has been validated using mathematical modeling as well as measurements taken during ALARA (As low as reasonably achievable) flight testing onboard the International Space Station [9]. This principle of large numbers of hydrogen atoms being able to shield will hopefully translate over to polyurethane foam. There are other promising single use materials such as Kevlar and Nextel. These materials are both used in structural application in current and future spacecraft. Both Kevlar and Nextel were the basis of the testing by Lobascio & Briccarello et al. They showed that Both Kevlar and Nextel provide more shielding in an accelerator based test than an identical mass of aluminum [10]. This is very promising as the base material for the subject composite is Kevlar. Their results of the ion testing are seen in Figure 3.

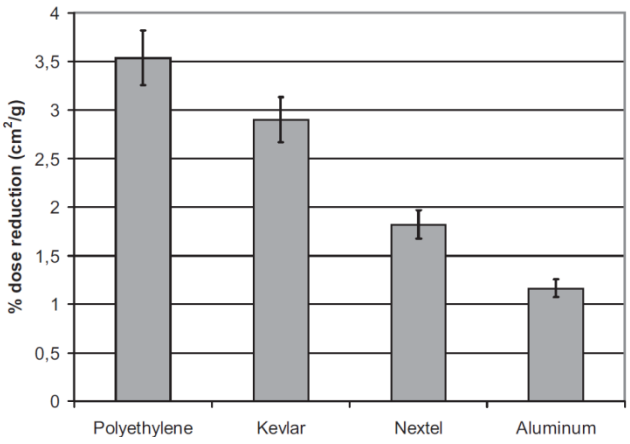


Figure 3: % dose reduction per density ($cm^2g^{-1}$) for 1 GeV Fe Ions extrapolated to zero thickness. [10]

## 2.3.Multi Layer Fluid Filled Composites

Considerable research has been done on Multi layer fluid filled composites considering the material has only been around for a short time. The material was created at New Mexico Institute of Mining and Technology in the late 2000's. The basic structure of the material is a skinned foam core composite [11]. The polyurethane foam core was bio inspired and originally thought of as a blast loading shield for masonry walls [12]. The cavities in the foam mimic the cavities in bone where marrow and blood pool. According to Matthews, bone contains approximately 25% liquid content and that liquid can help dampen mechanical loadings. The blood and marrow act as a significant dampening agent if the loading is above 1MHz, however they do show lesser effectiveness in the 0.2-1MHz range as well. Matthews constructed both flat and curved ½ inch thick polyurethane foam samples. The samples included both wet and dry foam. The samples were exposed to controlled explosive blasts as well as Split Hopkinson bar testing in the lab. The results showed that while the non fluid filled foam performed well, the fluid filled polyurethane consistently had a much higher modulus and less strain.

Matthews's research was continued by his research advisor Dr. Ghosh as well as a team from New Mexico Tech. The work by Ghosh et al focused on adaptive and stealth naval work. The basis of this work was to show that an engineered layer could have a higher acoustic transmission loss than acoustic mass law predicts. The additional dampening comes from the complex interactions between the fluid and the polyurethane foam cells [11]. Additionally more work was completed to further the dampening characteristics that were shown in Matthews's research. The Ghosh team also proposed putting a skin layer on their foam for greater adaptability and survivability in the naval environment. Multiple fabrics were considered based on desirable properties, these included Carbon Fiber, Nomex, Kevlar, fiberglass and Ballistic Nylon [11]. The researchers narrowed down the materials to Carbon fiber weave and multiple

weaves of Kevlar based on their respective properties. These materials were tested per ASTM D3039; each material sheet was cut into multiple coupons of differing geometries to quantify the strength differences. After extensive testing the Kevlar layers performed better in terms of strength and flexibility. The fluid filled composite material was then constructed and tested for multiple uses. The acoustic and dampening testing done by the Ghosh team was then expanded by graduate student Naitram Birbahadur. Birbahadur focused on repeating and then expanding on the testing that Matthews had done on just polyurethane foam [13]. In these tests, he was able to verify that the dynamic modulus of the material increased as the strain rate increased. This could lead to further research with the composite being used not only as a radiation shield but also as a barrier for high speed space debris and vibration suppression.

## 2.4.Multi Layer Fluid Filled Composites for Radiation Protection

There are no currently visible projects utilizing a fluid filled multi layer composite for radiation shielding. This was to be expected as New Mexico Institute of Mining and Technology holds the patent for the base material. Therefore a sizeable gap in understanding has been found and will be filled by this research.

CHAPTER III

# 3. Research Hypothesis, Objectives and Goal

## 3.1. Hypothesis

A composite material consisting of Kevlar faces and Polyurethane core can be suitably modified to survive in a high Gamma environment and will afford an elevated level of shielding.

## 3.2. Objective and Goal

This research will aim to select constituent materials that can be added to a basic Kevlar/polyurethane composite to increase both its shielding and survivability capabilities. The next objective would be to investigate the feasibility of creating such a composite material. The final objective would be to construct and test the composite material after it has been exposed to different levels of Gamma irradiation. The goals would be to show that the material can survive in a representative Gamma environment and provide some shielding. The material will be considered failing when its strength drops below 50% of its control group strength level.

CHAPTER IV

# 4. Approach

## 4.1.Material Selections

Based on positive results in the research on multilayer fluid filled composite work by Ghosh, Matthews & Birbahadur the composites will all contain the following: Kevlar, Epoxy, & Poron® Foam at a minimum.

Knowing that lead is classified as a heavy metal, other heavy metals were reviewed and investigated. These include the following elements: Iron, Boron, Cobalt, Copper, Manganese, Molybdenum, Zinc, Mercury, Plutonium as well as many others that are very rare and not suitable for this project. The last two materials on this list (Mercury & Plutonium) are very toxic materials and should not be used for any application that has human contact. Another consideration is that Plutonium is radioactive and would be emitting radiation from inside the material therefore hindering any shielding performance we may have gained. Boron was selected for further examination since it is a relatively lightweight element and can form very stable compounds that withstand harsh environments. The first and one of the most common compounds that comes to mind is borosilicate glass (Pyrex®) which can withstand very high temperatures and very fast temperature changes without breaking.

There were two options to introduce the boron into the material. The first was to include a boron-compound into the interstitial voids between the poly spheres. This would allow for the boron to have a relatively large volume while introducing no noticeable change in the overall dimensions of the material. This addition would not add any static structural

strength to the material but should also not hinder its movement as it will be in a dynamic environment.

The second option would be to include a borosilicate glass fiber into the composite either in the skin layer or in the foam layer. For ease of manufacture, the skin layer or an intermediate layer would be easiest as getting the fibers into the foam would present another set of challenges.

The boron compounds were both characterized in SRIM – Stopping and Ranging of Ions in Matter program which will be further discussed in section 4.3. After repeated results as reflected in Figures 5 & 6, the combination of Boron and Nitrogen was shown to have one of the better performances. The B-N material stopped ions with greater efficiency than the other compound. Looking into all B-N compounds and their crystal structures and material properties, Boron Nitride was selected as the interstitial compound that would be tested as it was the simplest in composition and lowest cost option with results similar to the higher complexity compounds.

Table 1: Boron materials and properties tested in initial simulation

| Candidate additives | Chemical Formula | Structure | Modulus (GPa) | Density (g/cm3) |
|---|---|---|---|---|
| Boron Nitride | BN | varies-hex, cubic | 100-400 | 2.28-3.49 |
| Borosilicate Glass Fibers | SiO2-B2O3-Na2O-Al2O3 | amorphous fiber | 62.75 | 2.23 |

## 4.2.Boron Selection

The B-N compound has multiple crystalline forms including cubic and hexagonal [14]. In its cubic form it has properties similar to that of diamond, not just as hard but also very stable in

thermal and chemical situations. The hexagonal form also mimics that of Carbon in the form of graphite as can be seen in Figure 4 below. It is very soft but also very stable; this makes it perfect for use as a wet flowing agent or lubricant. This flowing ability aligns it well with the need of the bulk material as it can be made very fine and fit within the poly material while it is being formed. [15]. The BN material may also be intermixed with water and the polyurethane matrix layer before the internal foam spheres are formed so as to coat the material within. The solution could also be soaked into the voids in the foam by mechanical means. This final procedure will be the method for this series of testing as there is no ability to manufacture the foam at New Mexico Tech.

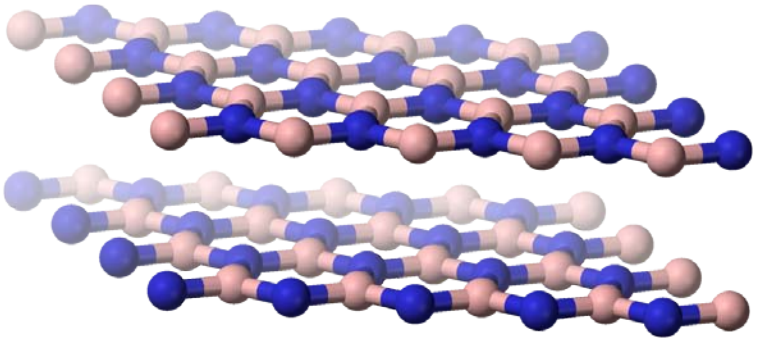

Figure 4: Boron Nitride in hexagonal form. Note similar structure to graphite sheets [14]

The second option to include boron in the material was to use a boron based fiber within the core of the composite. This option would give greater transverse strength to the material as the fibers would act as tension members. The fibers could be weaved into a cloth much the same as the Kevlar is. This would give a solid layer of boron based material; however it also directly affects the thickness of the material to the point where it could be the limiting factor if size is a major manufacturing issue. The boron based material should most likely be

borosilicate glass fibers as they can be weaved into a layer that is flexible as opposed to a stiff bulk material. This is a relatively well known type of fiberglass that is used in the construction industry as insulation as well as in many other scientific applications including ion stoppage [20].

## 4.3. Material Simulations in SRIM

The SRIM program, specifically the TRIM (Transport of Ions in Matter) module is based on the Monte Carlo simulation methodology. The version of the program used was SRIM 2011 Calculation 15. The software is available for free at www.SRIM.com. It specifically utilizes free flight path between ion collisions and only evaluates collisions that it deems significant. It also utilizes an analytical formula for calculating atom-atom collisions. The computer program outputs a max depth of penetration, it can output plots showing the bulk of the ion dissipation and other user defined plots [16]. The dissipation/depth plots can be seen in numerous figures including Figure 5. In the experimentation conducted, the target materials, penetrating ions, energy level, angle of incidence, and material thickness were varied. Each case was then compared with the same parameters between the candidate materials and only the most relevant plots are shown. The specific tests/simulations were modeled as they have a direct relationship with real world radiation situations. Throughout the testing the series will be explained.

Running the calculation simulations with a low number of ions, ranging from 1 to 100, but with high energy, 10-150 MeV shows that the interstitial boron nitride performs equal to the Borosilicate fibers at stopping the ions, but the fiber borosilicate material is more efficient at scattering them. This excess scattering can be seen in the following two figures (Figure 5 & 6). The first, Figure 5, is for 100 hydrogen ions with energy of 10 MeV contacting solid Boron Nitride

material. The second, Figure 6, is the same quantity hydrogen ions (100) with equal energy impacting fibrous Borosilicate. The scattering can be clearly seen compared to the BN material. Figure 7 shows the depth of penetration of the ions and their distribution in the foam with BN material. This is a different view that shows numerical distribution as opposed to figures 5 & 6 that show path of travel and distribution cannot be easily inferred.

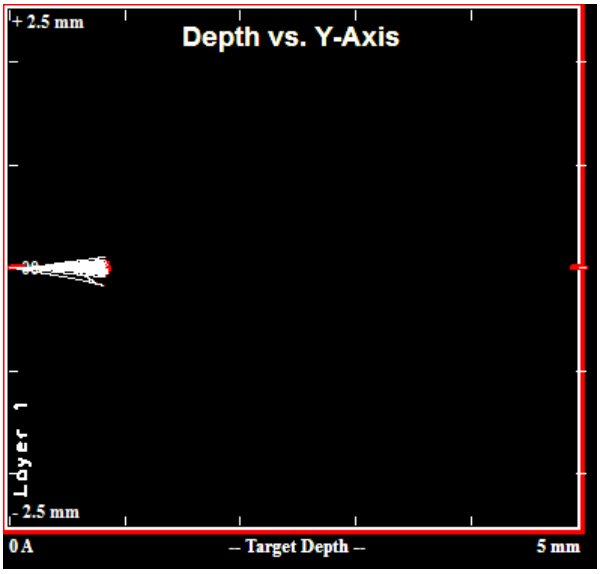


Figure 5: Hydrogen @ 10 MeV into Boron Nitride 5mm thick

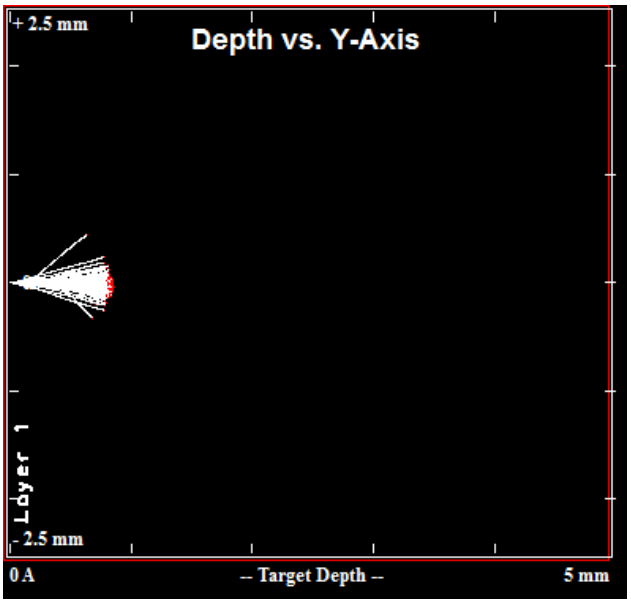


Figure 6: Hydrogen @ 10 MeV into 5mm Borosilicate material. Note excess scattering attributed to additional metal/heavy elements

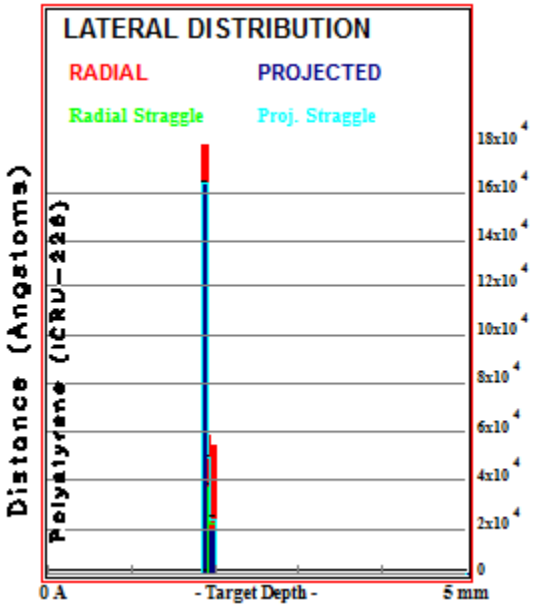


Figure 7: SRIM distribution of ions at 100 KeV in the interstitial boron nitride material.

Final material determination is made through material optimization calculations that lead to a determination of the minimum thickness of each layer of the material. At that time the penetrating ions will be varied by type and energy level; currently the penetrating media

are: Hydrogen which represents alpha particles, Helium representing Beta particles and Krypton representing the Gamma level energy.

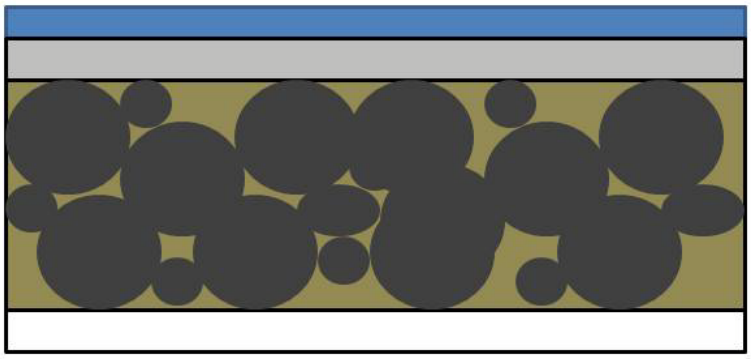

**Figure 8: General material layout, blue is Tyvek, light grey Kevlar, grey spheres polyurethane/$H_2O$, tan matrix is Boron Nitride and white is a cloth material for user comfort.**

## 4.4. Testing

The material shown above was run through calculations in the SRIM (Stopping and Ranging of ions in Matter) program with values based on the gamma ray energy greater than 100 KeV. The electron volt (eV) is a unit of energy based on a potential difference of one volt [18]. Iterations were completed with the following energy levels: 10MeV, 50 MeV, 75 MeV and 100MeV. The chosen numbers were very high as to witness what its protection limits were. In certain instances the material was subjected to only one ion so that a trace could be completed to see how well the material scattered the ion. The following two diagrams, Figure 9 & Figure 10, show the scattering caused by lead and by aluminum when subjected to the same number of Cobalt ions with identical energy. Note that the lead scatters the impact ions by a factor of ~2.25x and stops them at a depth of 2/3 of that of the aluminum. In limited instances, the impacts within the lead actually reverse direction.

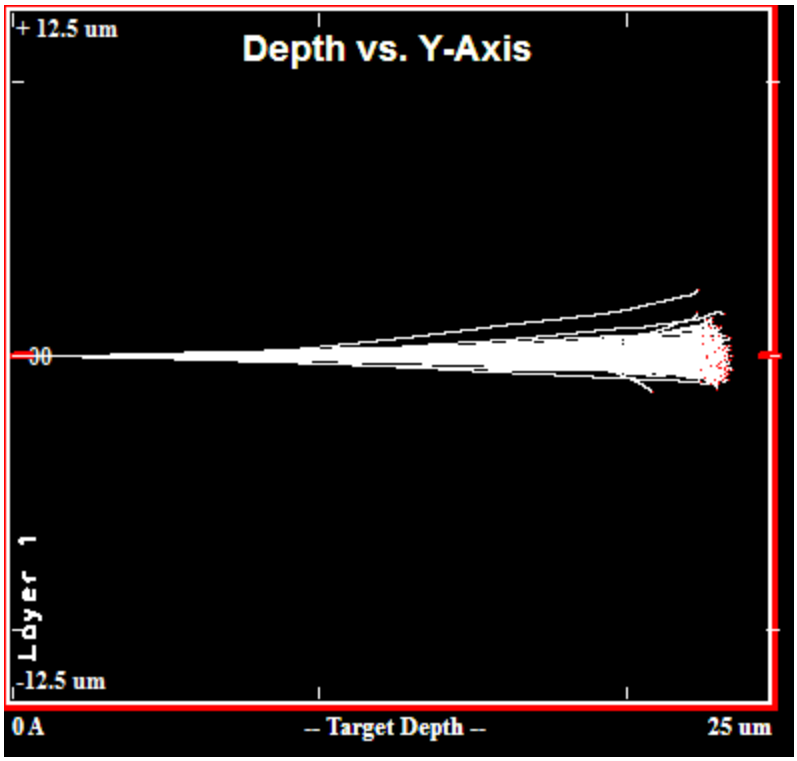


Figure 9: Cobalt in Aluminum 150,000 KeV

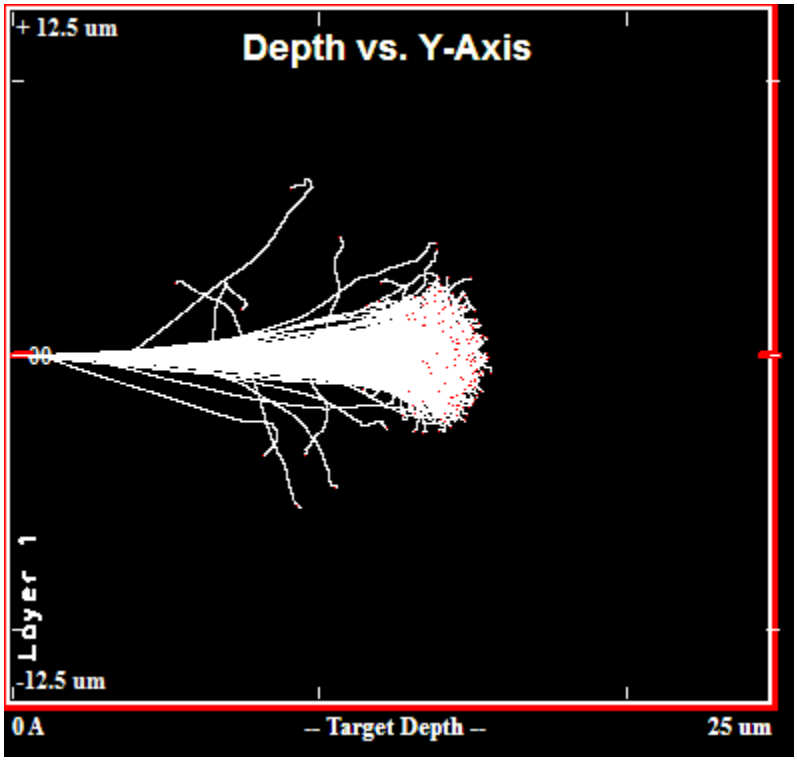


Figure 10: Cobalt in Lead 150,000 KeV

The figures below show just a sample of the material testing that was completed. In addition to the ion penetration plots, a plot of ionization and phonon location are included for critical instances. The ionization plots are a measurement of how much the ions change the base material structure whereas the phonon plots show the locations affected by phonons. Phonons are the induced forces that cause excess normal vibration within a material lattice structure.

### 4.4.1. Hydrogen Series

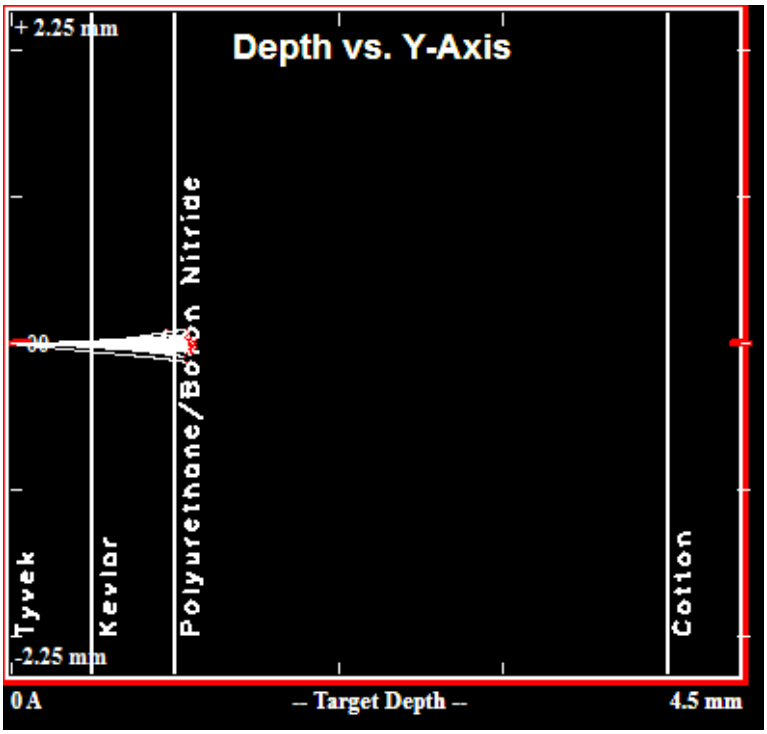


Figure 11: Hydrogen @ 10 MeV into FFMLC

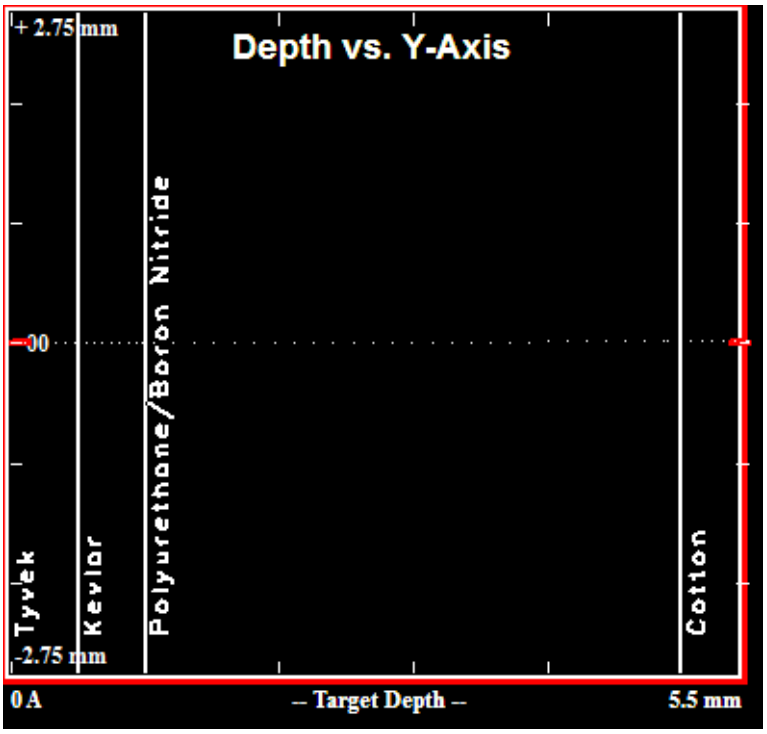


Figure 12: Single Hydrogen Ion @75 MeV into FFMLC

Figure 11 shows that the material is able to stop a large number of hydrogen atoms in the 1-1.25mm range. This simulation is very promising as it is within the normal gamma radiation power levels. Figure 12 shows a single ion at a total energy of 75 MeV, the single ion was used to gauge the slowing/stopping potential of each material in the composite. The Tyvek and Kevlar does not stop the ions as well as the Polyurethane/Boron Nitride segment did. Plots 13 & 14 show the phonon creation within the material; these plots show the location and magnitude of the ion recoils or ion collisions that result in an abrupt change in direction as well as the ionization created. As you can see in figure 11 the two largest energy loss points were within the Kevlar and polyurethane/B-N layer. The ions passed almost cleanly through the Tyvek layer as evidenced by the minimal scattering. However, the Tyvek does slow down the ions to some extent as can be evidenced by running the same test without the Tyvek. The

Kevlar layer gradually scatters the ions and finally they are scattered and stopped in the Poly layer.

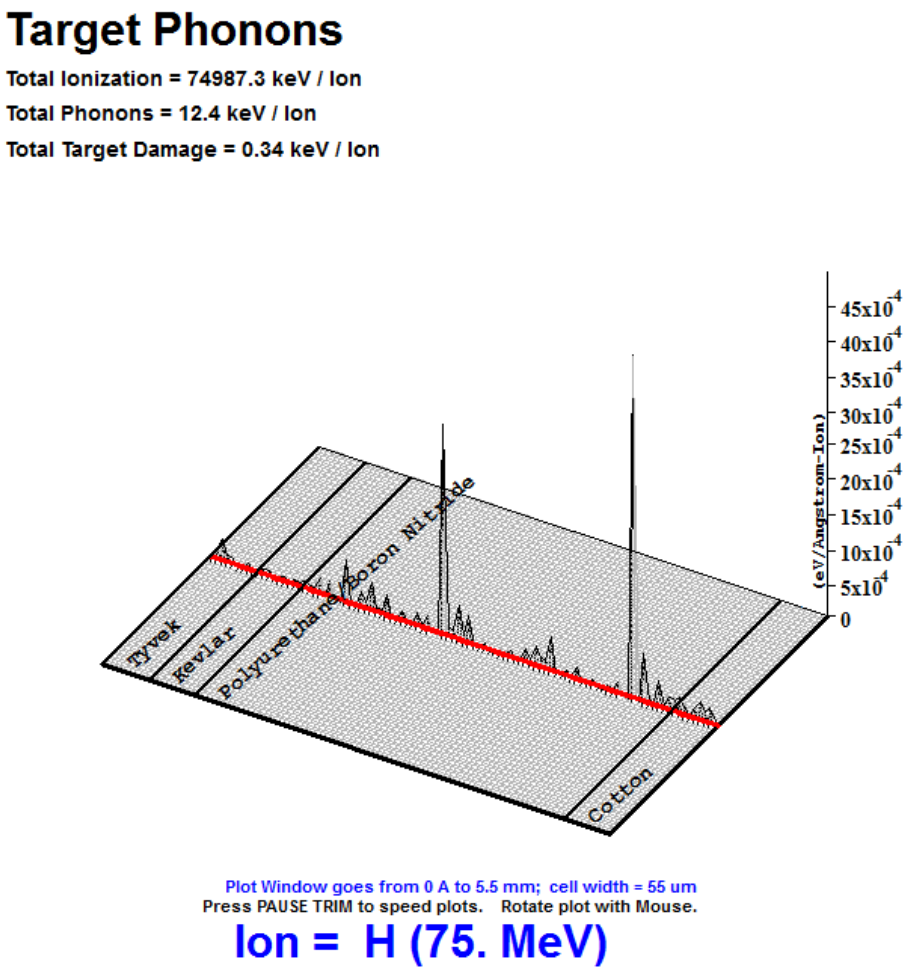


Figure 13: 3 Dimensional plot of Hydrogen phonon distribution @ 75MeV initial energy

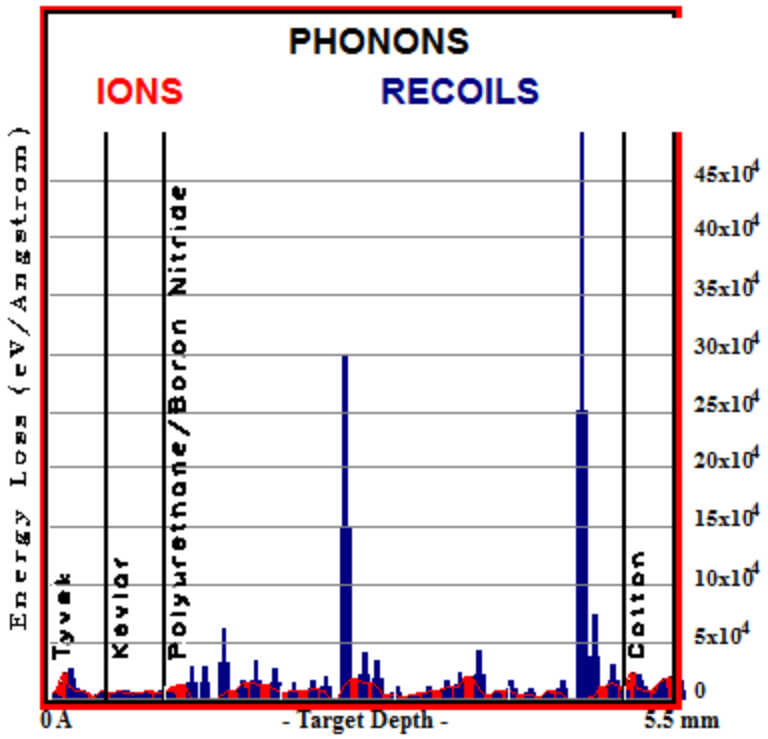


Figure 14: Phonon and energy loss plot for Hydrogen @ 75 MeV

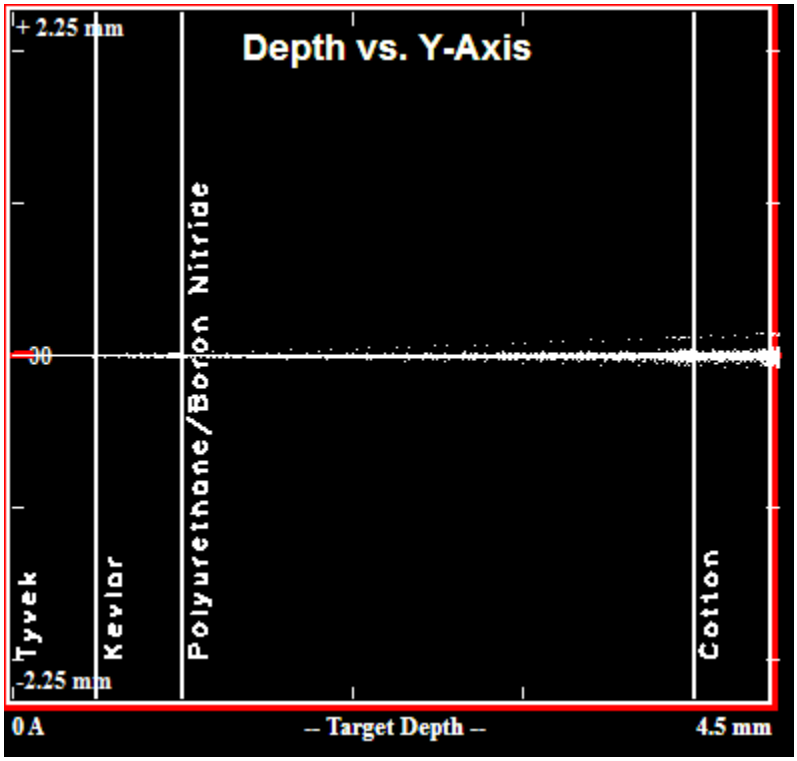


Figure 15: Hydrogen ions @ 100 MeV into the FFMLC. Note the complete penetration of the ions.

Figure 15 shows a complete overload of the material; the Hydrogen ions at 100 MeV potential pass completely through the material and this should be considered a failure of shielding. For this material a limit of less than 75 MeV should be exercised if it is subjected to Hydrogen ions.

### 4.4.2. Helium Series

The Helium series is very similar to the hydrogen series that was investigated earlier. Helium simulations are used as Helium is the product of nuclear fusion of two Hydrogen atoms. The biggest difference in the two is that the Helium ions are much bigger than the Hydrogen and tend to keep their momentum longer; however, since they are bigger they tend to impact the larger atoms inside the material more and can be somewhat easier to stop. Figure 16 shows us the impact of Helium at 10 MeV, this impact doesn't even penetrate completely through the Tyvek ® layer of the material. When we increase the momentum to 50 MeV, as seen in figure 16, the ions penetrate through the Tyvek and Kevlar but are stopped by the Polyurethane/B-N layer in the ~2mm range. Once it reaches the 75MeV a much shorter distance and greater stopping power is seen comparing the Helium ions in Figure 18 to the single Hydrogen Ion in Figure 12. Moving on to 75 MeV in the lower density core material shows that the ions not only travel farther in the material but also do not bounce as effectively nor veer off their straight line course.

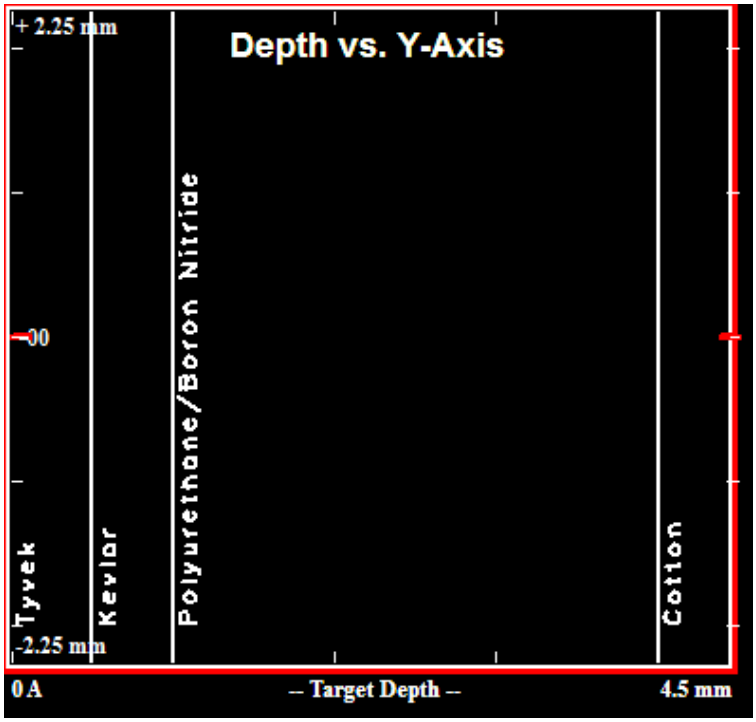


Figure 16: Helium @ 10 MeV into FFMLC. Note: Ions only penetrated to "00" mark at about .05mm

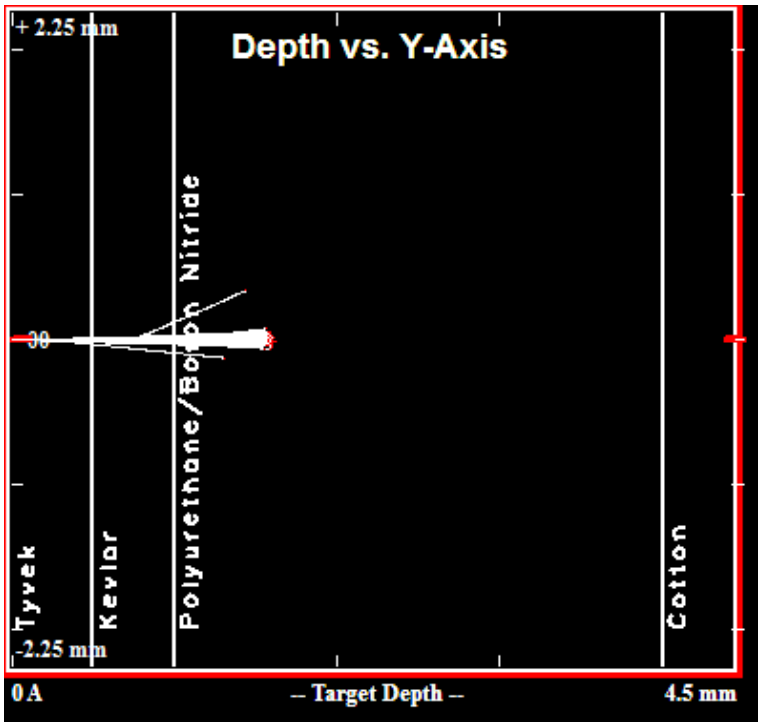


Figure 17: Helium @ 50MeV into FFMLC

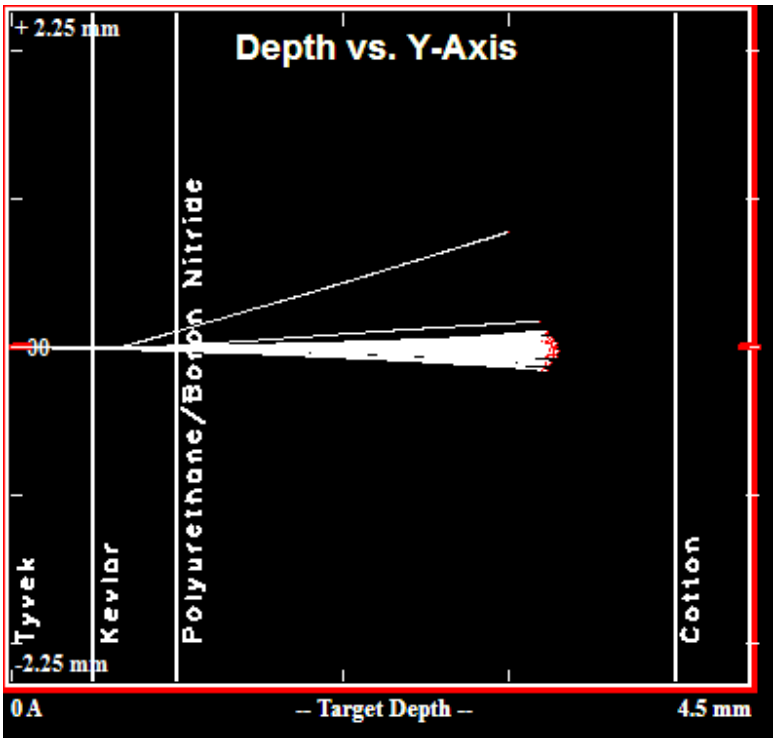


Figure 18: Helium at 75 MeV into FFMLC

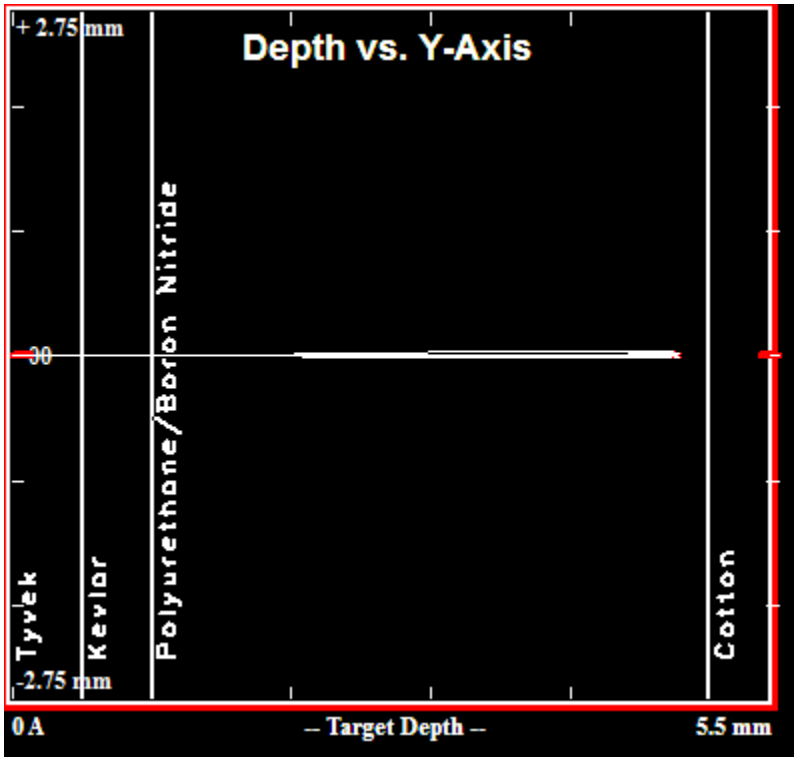


Figure 19: Helium @ 75 MeV into FFMLC with reduced density within the polyurethane layer of 3.5g/cm$^3$

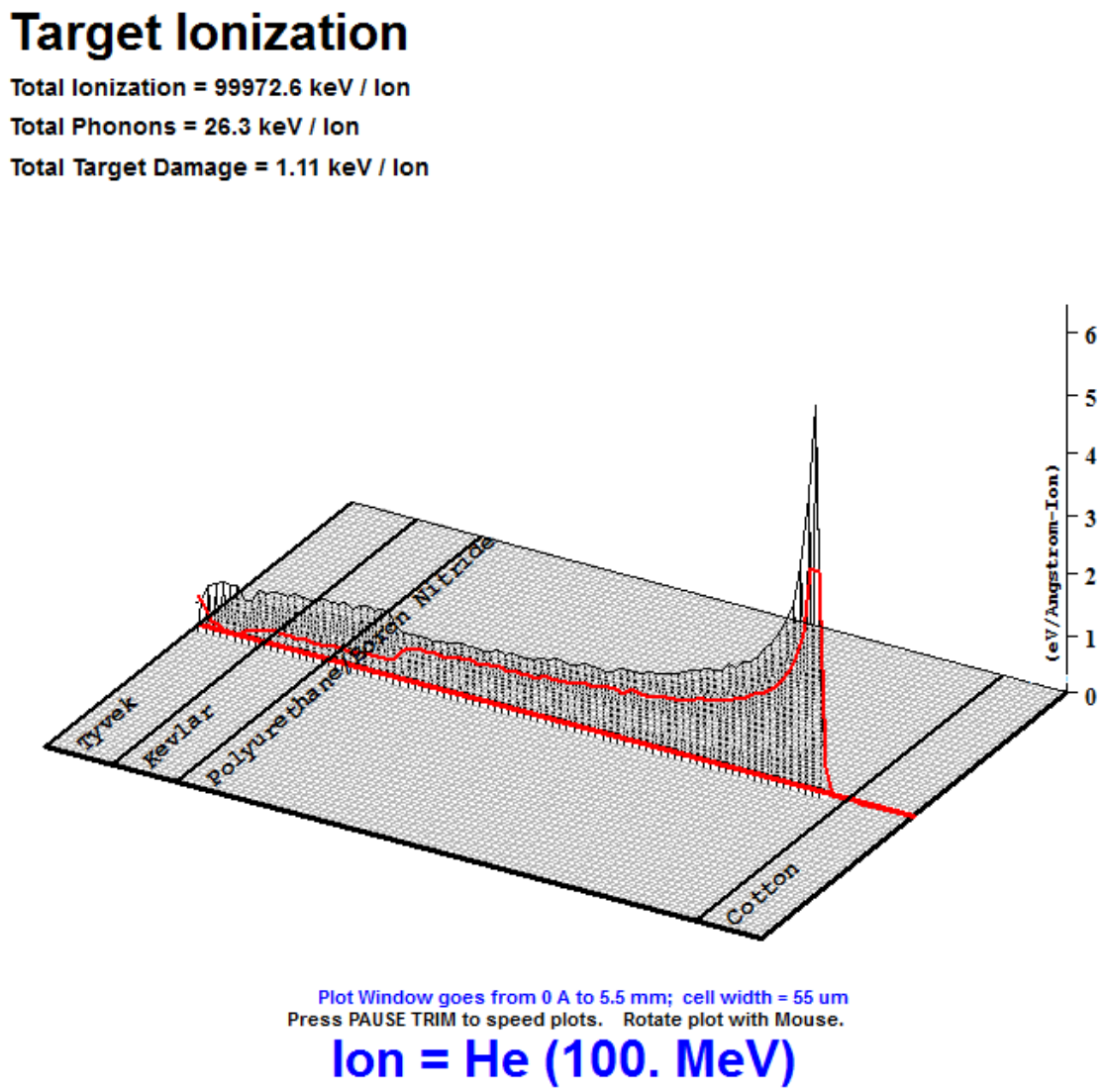


Figure 20: Ionization of the reduced density FFMLC. Note that the ionization did not pass into the cotton layer.

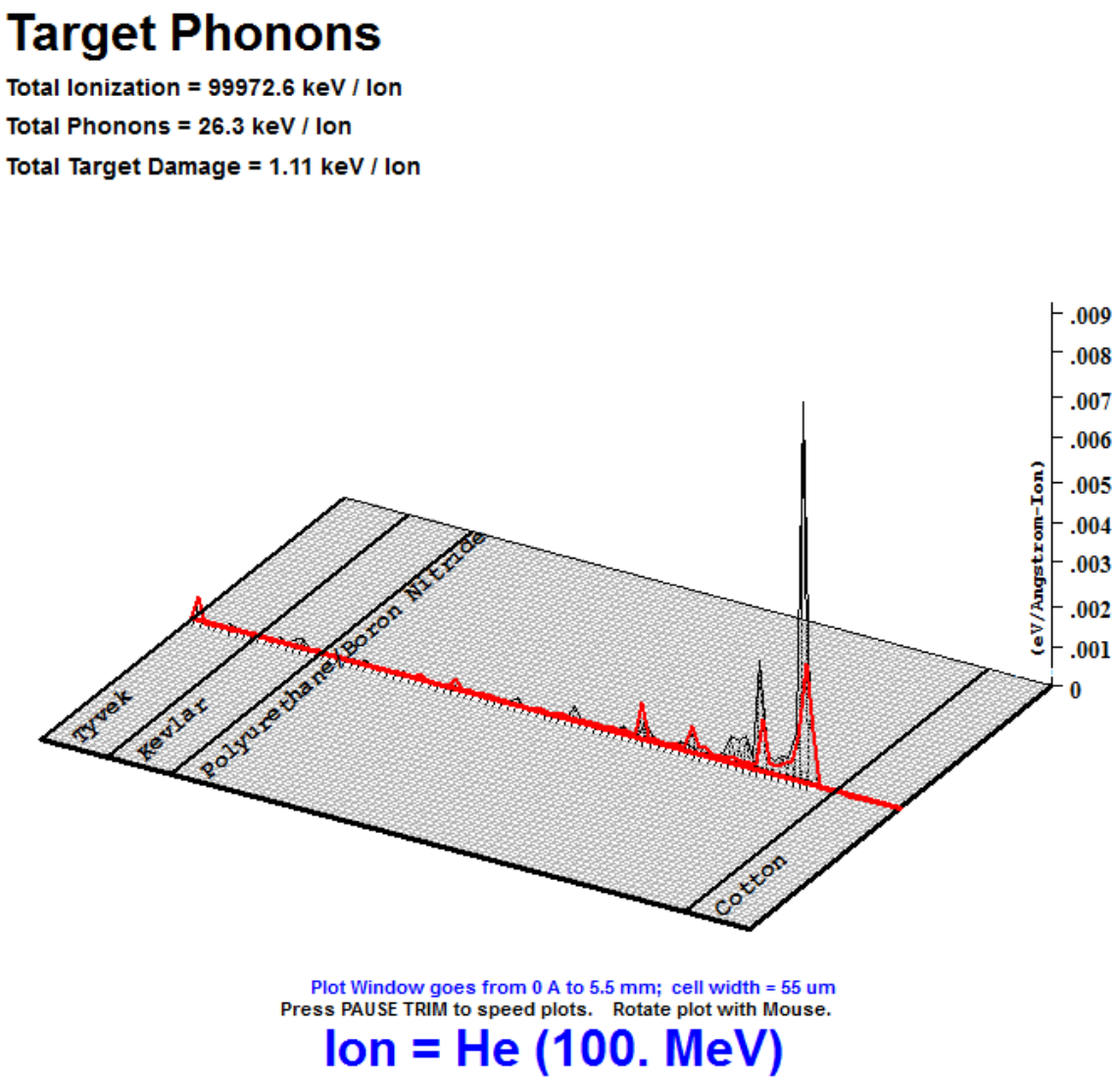


Figure 21: Phonon distribution of Helium @ 75MeV into Low density FFMLC.

Figure 20 & 21 show the Ionization and Phonons and both exhibit better performance than the Hydrogen series. The plots look very similar. However, the Helium series plots are for 100 MeV and the Hydrogen are only for 75MeV. Although the energy of the ions is higher the major phonon area is still within the polyurethane layer which means the wearer will not be subject to phonon energy in any layer below the composite layer, thus protecting their undergarments or skin. In figure 22 it can be observed that helium ions with a momentum of

100 KeV are able to fully penetrate the composite; once again this means we will have to limit our performance to less than 100MeV of energy.

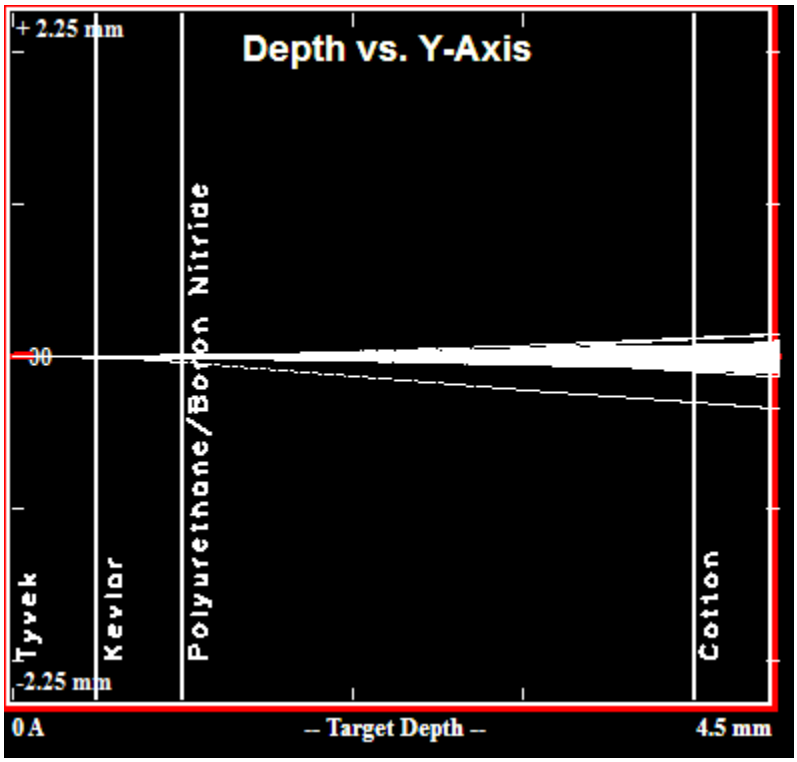


Figure 22: Helium @ 100 MeV into normal density FFMLC. Note complete penetration.

Based on the simulation testing, the Tyvek/Kevlar/Polyurethane/BN composite significantly reduces the amount of energy that passes through it. As the thickness of the poly layer is increased more protection can be afforded, but it also adds more weight and cost. The optimized thickness is approximately 5.5 mm which is thin enough to be manufactured and maneuverable but thick enough to provide adequate energy suppression.

## 4.5.Material Selection for Testing

The materials that will be considered for testing are Kevlar, Poron foam, Tyvek, Distilled Water (for purity) & BN solution. The base material will be Kevlar skinned Poron foam. The variables will be adding a layer of Tyvek, adding $H_2O$ or BN Solution. The table below lists the final combinations of materials.

**Table 2: Test Sample numbering and constituent materials**

| Sample | Layout |
|---|---|
| 1 | Kevlar/Poron/Kevlar |
| 2 | Kevlar/Poron/Kevlar |
| 3 | Kevlar/Poron/Kevlar |
| 4 | Kevlar/Poron/Kevlar |
| 5 | Kevlar/Poron/Kevlar |
| 6 | Kevlar/Poron/H2O/Kevlar |
| 7 | Kevlar/Poron/H2O/Kevlar |
| 8 | Kevlar/Poron/H2O/Kevlar |
| 9 | Kevlar/Poron/H2O/Kevlar |
| 10 | Kevlar/Poron/H2O/Kevlar |
| 11 | Kevlar/Poron/BN/Kevlar |
| 12 | Kevlar/Poron/BN/Kevlar |
| 13 | Kevlar/Poron/BN/Kevlar |
| 14 | Kevlar/Poron/BN/Kevlar |
| 15 | Kevlar/Poron/BN/Kevlar |
| 21 | Tyvek/Kevlar/Poron/Kevlar |
| 22 | Tyvek/Kevlar/Poron/Kevlar |
| 23 | Tyvek/Kevlar/Poron/Kevlar |
| 24 | Tyvek/Kevlar/Poron/Kevlar |
| 25 | Tyvek/Kevlar/Poron/Kevlar |
| 26 | Tyvek/Kevlar/Poron/BN/Kevlar |
| 27 | Tyvek/Kevlar/Poron/BN/Kevlar |
| 28 | Tyvek/Kevlar/Poron/BN/Kevlar |
| 29 | Tyvek/Kevlar/Poron/BN/Kevlar |
| 30 | Tyvek/Kevlar/Poron/BN/Kevlar |

In addition to these composite materials, a set of Kevlar skins and a set of Poron foam will be subjected to exposure. Samples 16-20 were originally going to contain Cerebrospinal

fluid but were removed due to material unavailability before Gamma exposure testing; the numbering continued using the originally designated system so all data would line up.

## 4.6.Experiment

The experiment will try and observe and quantify the damage done by varying amounts of radiation on multiple variations of discussed composite material.

### 4.6.1. Multi Layer Fluid Filled Composite Creation

As discussed above and shown in Table 2, there will be multiple test samples. The samples will be fabricated in a manner similar to that in previous experiments so as to be able to directly apply results to identical materials. The procedure from "A Novel Material…" will be followed and deviations will be noted and discussed.

The first step after reviewing the previous reports was to procure the materials needed. Step two was to smooth out the Kevlar fabric as when it was shipped it was folded and had wrinkles that can be seen in the picture below. The wrinkles in the fabric were removed with light hand pressure and utilizing a roller with light pressure.

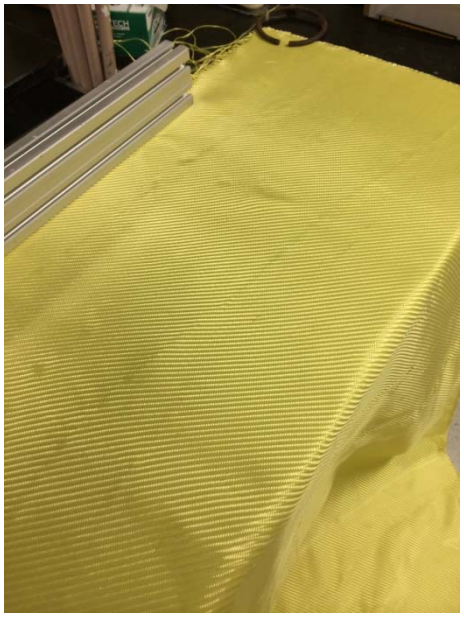

Figure 23: Kevlar fabric after being removed from packing material and before wrinkles were pressed out.

The next step was to mix equal parts of the resin and hardener for 5 minutes. 8 ounces of each were measured and placed in individual containers and then combined in a larger mixing bowl.

Figure 24: Epoxy Hardener on left and Resin on right prior to being mixed.

Figure 25: Epoxy mixing bowl after 5 minutes of vigorous mixing.

Once the epoxy was mixed thoroughly, it was spread evenly over the Kevlar sheeting which had a plastic sheet below it. The deviation was made so that all samples would have pregnated Kevlar/epoxy that was identical in consistency as well as curing temperature and curing rate. This would alleviate any concerns about different thicknesses and differences in material strength based on epoxy mixture and curing environment. The temperature of the room was 62 degrees and was kept at this temperature for the duration of the pregnating process.

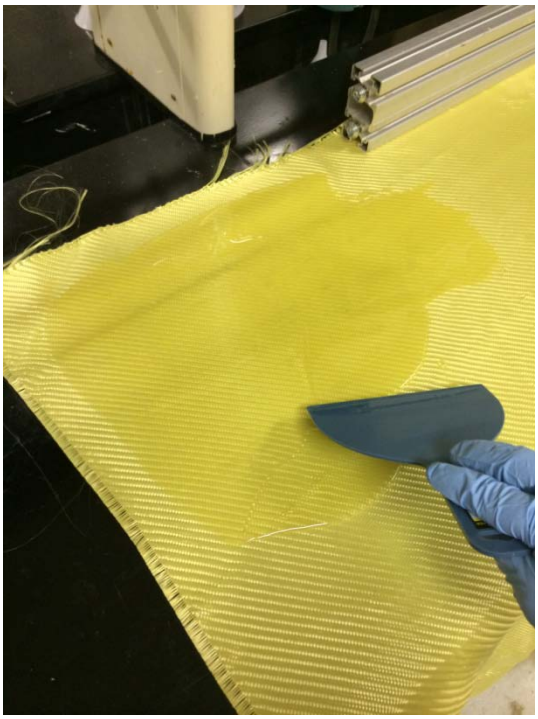

Figure 26: Kevlar mat being hand pregnated with epoxy.

While the Kevlar was left to cure, the Poron polyurethane foam was removed from its packaging and measured into 6” by 6” squares. The 24” x 24” marked Poron sheets were then cut with a new razor blade knife along a cutting guide to ensure crisp edges.

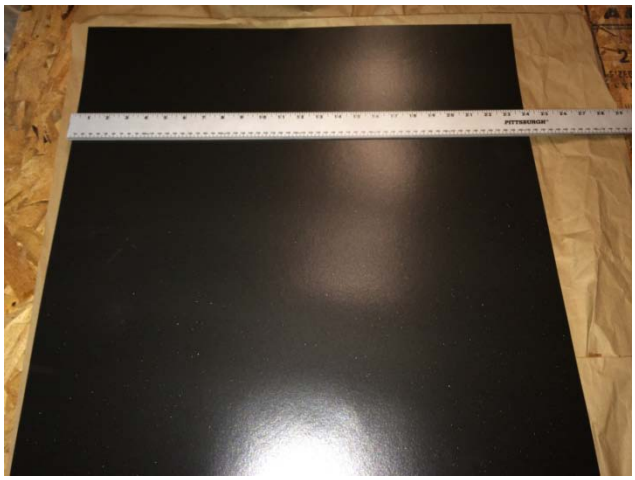

Figure 27: 24" x 24" Poron foam being measured prior to being sectioned.

After being sectioned, three of the Poron foams edges were coated with white silicone. The fourth side would remain open in order for liquid to be inserted into some of the samples. This procedure was dome so that the Poron foam would act like a cup once it was filled and no liquid that was added could leak out while the tope was being sealed. This was the best option at the time but later this decision will be reversed.

Figure 28: Poron foam squares with silicone applied to the sides before it was smoothed out.

The silicone was spread out on the edges and left to dry overnight in the same room as the Kevlar sheet. The next morning the Kevlar sheet was sectioned into 7” wide sheets using an edge guide clamp and razor blade knife. The strips of Kevlar were then placed on top of wax paper so they would not stick to the work table. The Poron samples that had previously been numbered were aligned with the Kevlar sheet to ensure that the top of each sample and the bottom of each sample had material with the same directionality.

Figure 29: Poron samples being aligned with Kevlar strips before being bonded.

The Kevlar strips were lightly sanded with 180 grit all purpose sandpaper to remove the sheen on the back of the sheet. This side was to be the side that is bonded to the Poron foam. The same epoxy mixture that was used to pregnate the strips was then made to coat the strips and bond to the Poron foam. The epoxy was applied to the face of the Poron foam with a plastic putty knife and spread evenly over the surface. The samples were then placed on the Kevlar sheet in the predetermined manner. The back of the Poron was then coated with an equal amount of epoxy and the Kevlar strip placed on top. A sheet of wax paper was then applied lengthwise over the sandwich so that it could be compressed without the epoxy sticking to the wood that was compressing it. Wood was used instead of aluminum plates as the aluminum stock on hand was not wide enough to cover the entire sample and was also very cold due to being outside. The samples were clamped to an average torque of 50 ft lbs to ensure uniform bonding. This torque on the clamps was enough to fully compress the foam without

damaging it or the Kevlar. The composite was left to sit for 12 hours at 62 degrees Fahrenheit to fully cure.

Figure 30:Clamped Kevlar/Poron composite.

Once removed from the clamp the composite looked like the sheet below showing sample 22, 25 and 24. It would later be sectioned by rough cutting on a band saw and be similar to sample 7 in Figure 31.

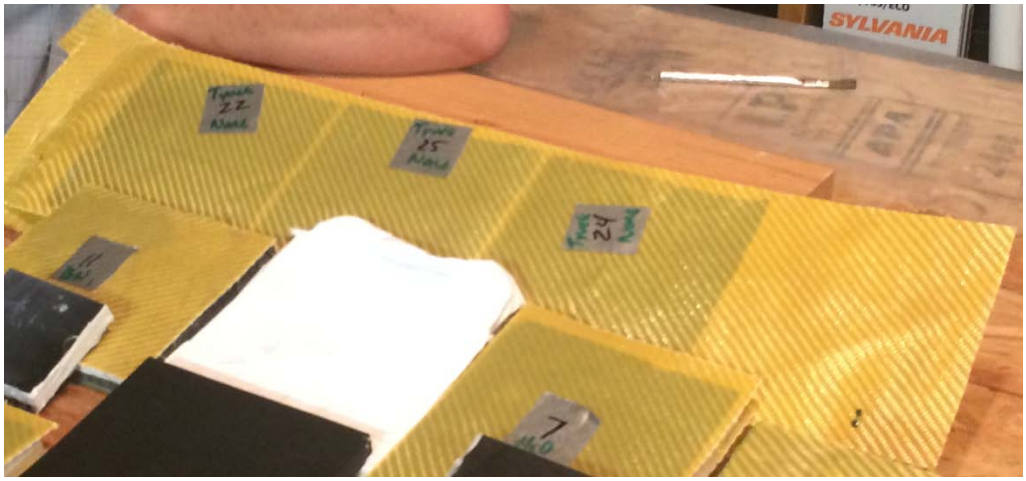


Figure 31: Collection of samples in strip form as well as others that had been sectioned.

The next step before final trimming on any of the samples was completed was to apply the Tyvek to the face of certain samples. This was completed by first lightly sanding the face of the Kevlar with 180 grit sandpaper and wiping clean with a damp cloth. Once the face was dry a layer of 3m 77 super spray adhesive was sprayed on the bonding face of the Tyvek and on the Kevlar face. The spray adhesive was allowed to sit for 1 minute per manufacturer's directions and then the faces were carefully bonded. The composite was then clamped at 30 lb ft to ensure a consistent bond. After 1 hour the materials were removed. The samples are shown in Figure 31, 32 and 33.


Figure 32: Backside of Tyvek Faced composites

Figure 33: Tyvek face after bonding with Kevlar composite.

The newly skinned materials were trimmed on a band saw to the initial 6”x6” dimensions of the Poron. A single spare test sample was weighed and then placed in a water bath in an attempt to fill it. The procedure of rolling a press over it originally discussed in J Matthews paper was only able to partially fill the composite [12]. This was based on the added weight when the material was weighed again. After calculating the before and after weight of

the samples only approximately 10 milliliters of water were added. The material was still full of air in the corners near where the sides were sealed. A new procedure was needed to fill the foam to a higher level. It was decided that the 3 sides with silicone on them would be trimmed on a band saw to allow water penetration and air exit from each of the sides. The test sample was cut first and then submerged using Matthews procedure. Even after only one test fill, the amount of water that was able to enter it was substantially greater. This process would be utilized for the remainder of the samples. All of the samples were trimmed on the band saw to approximately 5.5" x 5.5 "and then weighed. The initial weights are listed in the table in the results section.


Figure 34: Trimmed test samples being weighed before filling with water.

Once a set of test coupons were complete they were placed in a tub containing their filling material. The process of filling each was the same no matter the liquid used to fill. Figure 35 shows the samples being placed in the distilled water bath. The water was warmed to 140°F

to allow it to warm the foam and flow more easily. Figure 36 shows the pipe being used to squeeze air our and allow water to be drawn into the composite. This was repeated 10 times in the X and 10 times in the Y direction to ensure maximum fill.


**Figure 35: A set of test coupons sitting in distilled water bath before filling.**


**Figure 36: Pipe being used to roll the composite and squeeze air pockets out and draw water in.**

Once each sample was filled it was allowed to rest underwater with an object over it to prevent it from floating for approximately 1 hour. This allowed any residual negative pressure to draw water in before it was weighed and then sealed. Each sample was removed from the

water bath and weighed on the digital scale quickly before any liquid escaped. The next step was to use a wet curable silicone to seal the wet edges of the foam. This was done by using GE Silicone II and drawing a bead along the edge and smoothing it out with a putty knife. As shown in figure 37. Once the samples had been coated they were weighed again and then placed on wax paper to allow the silicone to cure overnight.

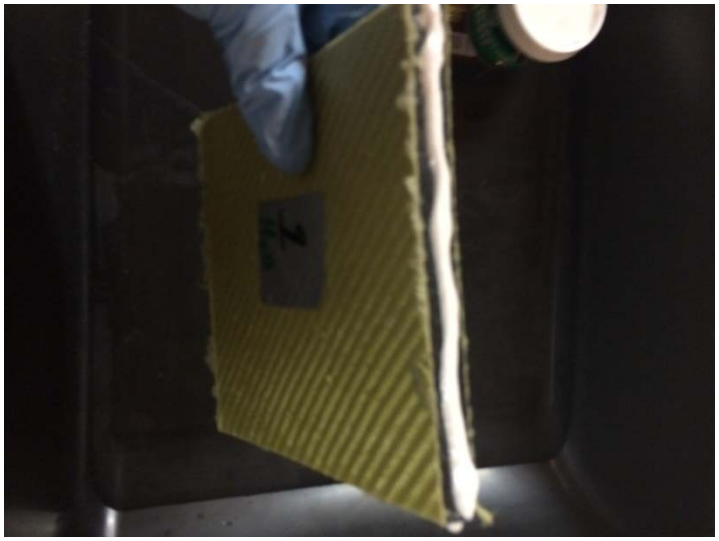

**Figure 37: Silicone being applied to the sides of the composite after being filled with liquid**

Figure 38: Filled samples with silicone curing.

The Boron Nitride solution was created using distilled water and a fine powder hexagonal Boron Nitride. 11 grams of Hex BN was mixed with 1.5 Liters distilled water.

Boron Nitride is 24.82 g/mol.

To find the molar concentration we must first find how many mols of BN we have by using the formula:

$$Mols = \frac{Test\ Mass}{Mass\ per\ Mol} = \frac{11g}{24.82\ \frac{g}{mol}} = .44\ Mols$$

We then divide the number of Mols of BN into the volume of water to determine the solutions molarity.

$$Molarity = \frac{Mols}{Volume\ of\ solution} = \frac{.44\ Mol}{1.5\ L} = .295$$

The BN solution was .295M when it was mixed. The solution was created using 140°F distilled water to allow for easier mixing and fluid entry into the foam. The procedure for inserting BN into the composite was the same as inserting water.

The samples were allowed to cure overnight and then weighed again the next morning to ensure there were no leaks in the composite. Once they were fully cured they were placed in a sealed airtight tub to keep external contaminants off of them.

The final material specifications are listed in the table below. As you can see the liquid filled materials were filled to approximately 80%. The samples were all slightly different in size and this attributed to the majority of the difference in liquid and dry weights. The calculation for the fill percentage data was taken from Matthews [12]. The "Approx Fill" column is the percentage of available pores filled.

**Table 3: Table showing wet weights and fill percentages of each composite.**

| Sample | Layout | Exposure | Group | Initial We | Wet Weig | 2nd Wet Weight | Silicone Wt | Wet Weig | Approx fill |
|---|---|---|---|---|---|---|---|---|---|
| 1 | Kevlar/Poron/Kevlar | 0 (Control) | 1 | 120 | 125 | 125 | 5 | 0 | 0.00 |
| 2 | Kevlar/Poron/Kevlar | 5 Gy | 2 | 123 | 129 | 129 | 6 | 0 | 0.00 |
| 3 | Kevlar/Poron/Kevlar | 50 Gy | 3 | 116 | 121 | 121 | 5 | 0 | 0.00 |
| 4 | Kevlar/Poron/Kevlar | 250 Gy | 4 | 111 | 116 | 116 | 5 | 0 | 0.00 |
| 5 | Kevlar/Poron/Kevlar | 500 Gy | 5 | 115 | 121 | 121 | 6 | 0 | 0.00 |
| 6 | Kevlar/Poron/H2O/Kevlar | 0 | 1 | 158 | 287 | 286 | N/A | 128 | 0.82 |
| 7 | Kevlar/Poron/H2O/Kevlar | 5 Gy | 2 | 128 | 252 | 251 | N/A | 123 | 0.78 |
| 8 | Kevlar/Poron/H2O/Kevlar | 50 Gy | 3 | 150 | 281 | 280 | N/A | 130 | 0.83 |
| 9 | Kevlar/Poron/H2O/Kevlar | 250 Gy | 4 | 121 | 239 | 238 | N/A | 117 | 0.75 |
| 10 | Kevlar/Poron/H2O/Kevlar | 500 Gy | 5 | 167 | 311 | 308 | N/A | 141 | 0.90 |
| 11 | Kevlar/Poron/BN/Kevlar | 0 | 1 | 131 | 257 | 255 | N/A | 124 | 0.79 |
| 12 | Kevlar/Poron/BN/Kevlar | 5 Gy | 2 | 146 | 274 | 273 | N/A | 127 | 0.81 |
| 13 | Kevlar/Poron/BN/Kevlar | 50 Gy | 3 | 147 | 275 | 274 | N/A | 127 | 0.81 |
| 14 | Kevlar/Poron/BN/Kevlar | 250 Gy | 4 | 125 | 248 | 247 | N/A | 122 | 0.78 |
| 15 | Kevlar/Poron/BN/Kevlar | 500 Gy | 5 | 115 | 235 | 235 | N/A | 120 | 0.77 |
| 21 | Tyvek/Kevlar/Poron/Kevlar | 0 | 1 | 122 | 127 | 127 | 5 | 0 | 0.00 |
| 22 | Tyvek/Kevlar/Poron/Kevlar | 5 Gy | 2 | 126 | 130 | 130 | 4 | 0 | 0.00 |
| 23 | Tyvek/Kevlar/Poron/Kevlar | 50 Gy | 3 | 131 | 137 | 137 | 6 | 0 | 0.00 |
| 24 | Tyvek/Kevlar/Poron/Kevlar | 250 Gy | 4 | 126 | 132 | 132 | 6 | 0 | 0.00 |
| 25 | Tyvek/Kevlar/Poron/Kevlar | 500 Gy | 5 | 133 | 139 | 139 | 6 | 0 | 0.00 |
| 26 | Tyvek/Kevlar/Poron/BN/Kevlar | 0 | 1 | 116 | 236 | 235 | N/A | 119 | 0.76 |
| 27 | Tyvek/Kevlar/Poron/BN/Kevlar | 5 Gy | 2 | 114 | 235 | 235 | N/A | 121 | 0.77 |
| 28 | Tyvek/Kevlar/Poron/BN/Kevlar | 50 Gy | 3 | 115 | 236 | 236 | N/A | 121 | 0.77 |
| 29 | Tyvek/Kevlar/Poron/BN/Kevlar | 250 Gy | 4 | 130 | 255 | 254 | N/A | 124 | 0.79 |
| 30 | Tyvek/Kevlar/Poron/BN/Kevlar | 500 Gy | 5 | 150 | 277 | 277 | N/A | 127 | 0.81 |

### 4.6.2. Gamma Irradiation of Composite & Constituent Material

The Gamma Irradiation Facility (GIF) at Sandia National Laboratories was utilized to expose the samples to elevated levels of Gamma Irradiation. The facility has 3 cells to expose samples to a Cobalt 60 gamma producing environment for any period of time. The test was conducted in Cell 3 which is one of the two smaller cells but at the time of testing had the highest dose rate based on the Cobalt 60 pin placements. There were 6 pins arranged in a circle as opposed to 3 in the other cell. The figure below shows the inside of GIF Cell 3 with samples as we were discussing alignment scenarios. The pool at the top of the picture is the water shielding pool that the Cobalt 60 sits at the bottom of. It utilizes an elevator to raise the Cobalt rods in a controlled manner.

Figure 39: GIF Cell 3 with samples placed at 200 cm during discussions on testing.

Based on research of radiation exposure while traveling to Mars and discussions with the subject matter experts, the dosage that the samples would be exposed to was changed slightly from initial discussions with Dr Ghosh. This change gave a larger range of values that were still based on the calculated mission to Mars exposure of 5 Gy per mission. A calculation of dose rate based on the pin alignment and distance from the emitter in the GIF cell was done to present us a starting point. Once the GIF staff completed this calculation they informed us a rate of 0.1 Gray per second could be achieved at a distance of 200 cm. This rate was sufficient for this test so dosimetry was put in the cell at the test distance to ensure that the calculated and measured value were indeed in agreement. The test samples were separated into 5 groups corresponding to the dosage they were to receive. The table below shows the groups. The groups were designed to give sufficient spacing without completely destroying the material.

Table 4: Grouping of materials to be exposed at GIF.

| Sample | Layout | Exposure | Group |
|---|---|---|---|
| 1 | Kevlar/Poron/Kevlar | 0 (Control) | 1 |
| 2 | Kevlar/Poron/Kevlar | 5 Gy | 2 |
| 3 | Kevlar/Poron/Kevlar | 50 Gy | 3 |
| 4 | Kevlar/Poron/Kevlar | 250 Gy | 4 |
| 5 | Kevlar/Poron/Kevlar | 500 Gy | 5 |
| 6 | Kevlar/Poron/H2O/Kevlar | 0 | 1 |
| 7 | Kevlar/Poron/H2O/Kevlar | 5 Gy | 2 |
| 8 | Kevlar/Poron/H2O/Kevlar | 50 Gy | 3 |
| 9 | Kevlar/Poron/H2O/Kevlar | 250 Gy | 4 |
| 10 | Kevlar/Poron/H2O/Kevlar | 500 Gy | 5 |
| 11 | Kevlar/Poron/BN/Kevlar | 0 | 1 |
| 12 | Kevlar/Poron/BN/Kevlar | 5 Gy | 2 |
| 13 | Kevlar/Poron/BN/Kevlar | 50 Gy | 3 |
| 14 | Kevlar/Poron/BN/Kevlar | 250 Gy | 4 |
| 15 | Kevlar/Poron/BN/Kevlar | 500 Gy | 5 |
| 21 | Tyvek/Kevlar/Poron/Kevlar | 0 | 1 |
| 22 | Tyvek/Kevlar/Poron/Kevlar | 5 Gy | 2 |
| 23 | Tyvek/Kevlar/Poron/Kevlar | 50 Gy | 3 |
| 24 | Tyvek/Kevlar/Poron/Kevlar | 250 Gy | 4 |
| 25 | Tyvek/Kevlar/Poron/Kevlar | 500 Gy | 5 |
| 26 | Tyvek/Kevlar/Poron/BN/Kevlar | 0 | 1 |
| 27 | Tyvek/Kevlar/Poron/BN/Kevlar | 5 Gy | 2 |
| 28 | Tyvek/Kevlar/Poron/BN/Kevlar | 50 Gy | 3 |
| 29 | Tyvek/Kevlar/Poron/BN/Kevlar | 250 Gy | 4 |
| 30 | Tyvek/Kevlar/Poron/BN/Kevlar | 500 Gy | 5 |

The control group was not exposed at the GIF. The groups were exposed at the levels listed in table 4. In order to be time efficient in the cells group 5 was combined with the other groups to achieve an aggregate exposure of 500 Gy as defined in the test matrix. When setup, group 5 was placed in the back corner of the cell as it would not be disturbed during the entirety of the testing, the other groups occupied space near the exit. Each group had dossimetry to validate the exposure it experienced post test. The dossimetry can be seen on the face of the samples in the following picture. The material used for testing will be taken from a different location to avoid any attenuation the dossimetry may have provided.

Figure 40: Test setup at 200 cm showing dosimetry on face of samples.

The samples were exposed in the following manner:

Table 5: Exposure table for each composite group.

| Groups | Exposure | Time (sec) | Time (min) | Cumulative for Group 5 |
|---|---|---|---|---|
| 2,5 | 5 Gy | 50 | 0.83 | 5 Gy |
| 3,5 | 50 Gy | 500 | 8.33 | 55 Gy |
| 4,5 | 250 Gy | 2500 | 41.67 | 305 Gy |
| 5 | 195 Gy | 1950 | 32.5 | 500 Gy |

The samples were allowed to acclimate to the test chamber overnight. This was done to ensure there was no thermal shock to the fluid filled composites. The next morning it was discovered that a few of the samples had fallen over due to failed mounting stands. This can be seen in figure 40 below. The picture was taken from the hallway of the cell via the mirror. The mounting stands were reinforced before testing began and no other anomalies were seen.

Figure 41: Photo showing two samples that had fallen overnight.

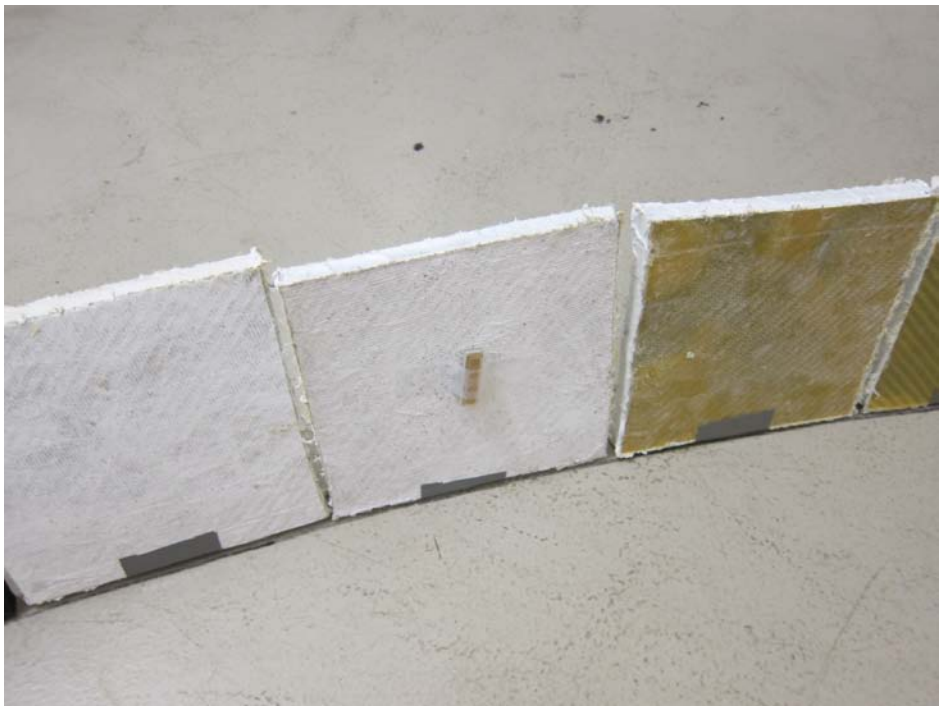

Figure 42: Dossimetry on face of test sample

Figure 43: Photo of test samples through ultra thick leaded glass window during exposure.

Once the samples were radiated in the prescribed order they were placed back in the airtight tub to be taken for weighing and mechanical testing.

### 4.6.3. Post Irradiation Testing

The samples will be evaluated by tensile testing. The testing will be in accordance with the specifications outlined in ASTM D3039. ASTM D3039 is titled "Standard Test Method for Tensile Properties of Polymer Matrix Composite Materials"

ASTM D3039 allows for tabs on the ends of the test coupons to be used if required [17]. In order to determine if tabs were needed two test samples were created from spare Kevlar material that was fabricated with the rest of the test samples. The samples were to undergo tension testing to determine if the failure point would be within the allowable area per ASTM D3039. Each test sample was 0.5 inches in width and the test area was 1". The sample that would have aluminum tabs on it was marked the 1" test length and then .050" aluminum sheet was sectioned to fit along the gripping area. The aluminum was coated with 3200 psi 5 minute epoxy on one side and the Kevlar was sandwiched between two pieces of aluminum. The sandwich was clamped for 30 minutes for the epoxy to fully cure. The final test coupons can be seen in figure 44.

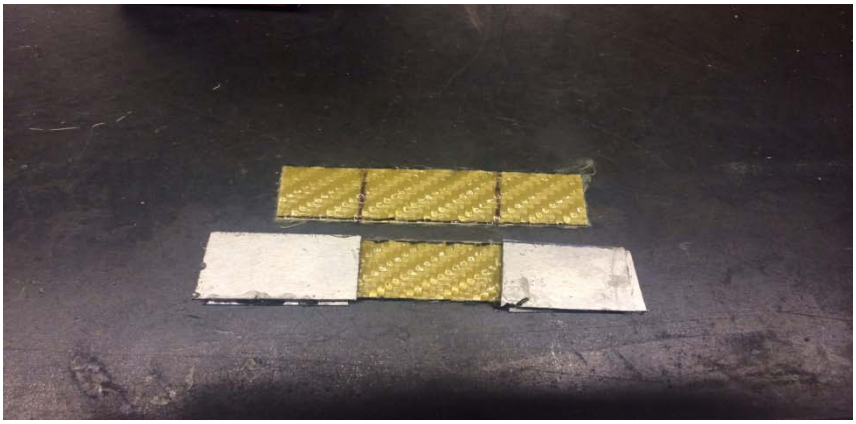

Figure 44: Test samples to determine the need for tabs on test samples

The samples were then individually loaded in the jaws of the MTS machine and clamped down to 100psi. The system was set to a constant head speed of .0656 in/min to correspond to the testing done by Ghosh et al. The aim of the test was not to look at the strength of the samples but where each sample failed. Both samples failed in the test area and based on that fact the actual test samples would be without gripping tabs.

The samples that were exposed to radiation and the control samples were then taken into the NMT Mechanical Engineering Machine shop and sectioned to approximately 1" wide strips. The samples were first cut to a straight edge to remove a side with silicone. Once the edge was clean and true a line was drawn 1" from the straight edge using a double square. The sample was then cut on a fine toothed band saw and set aside. Once all samples had been sectioned, the foam in the middle was cut in half to leave a face side and a rear side with foam. The samples were then individually mechanically stripped of the foam on the back of the Kevlar. Initially the foam was removed by using a razor blade until only a fine layer of foam was left. The remainder of the foam was removed using a plastic abrasive brush. Finally, 60 grit sandpaper was used to remove any remainder. Once the samples were complete they were taken into the lab for testing. The completed rear Kevlar samples can be seen in the figure below.

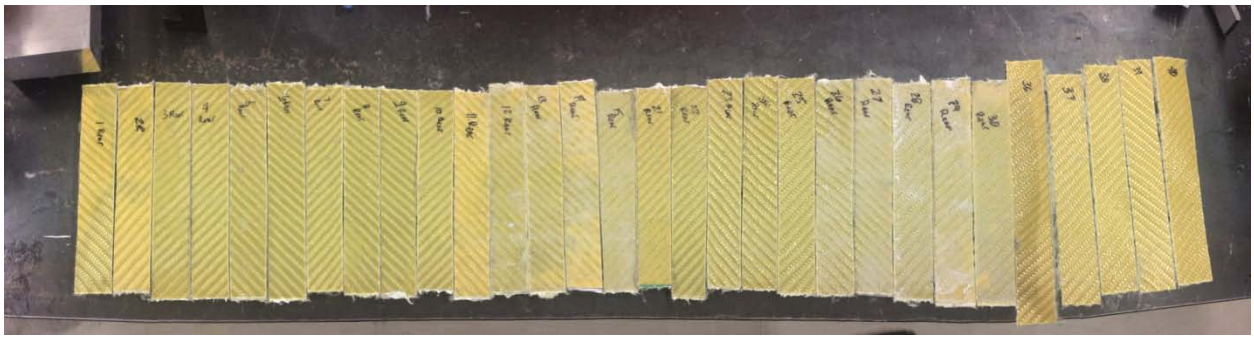

Figure 45: Completed 1" wide test coupons.

The samples were tested on the MTS Landmark 370 uniaxial tensile test machine seen in figure 46. The unit is electronically controlled and hydraulically powered; the hydraulic unit can be seen in figure 47 with the control station directly behind it.


**Figure 46: MTS Landmark 370 uniaxial test stand used on Kevlar samples.**

Figure 47: MTS Landmark Hydraulic power unit.

The samples were individually loaded into the jaws that were preset to a test length of 3 inches. The sample was aligned with marks on the machine and the guides that were preset to ensure the sample was perfectly aligned with the direction of tension. This can be seen in figure 48. Once the sample was fully aligned the jaws were clamped to a pressure of 100 psi. This pressure was chosen as it did not allow the preliminary test samples to slip and also avoided crushing the clamped area. Before the samples were stressed they resembled figure 49.

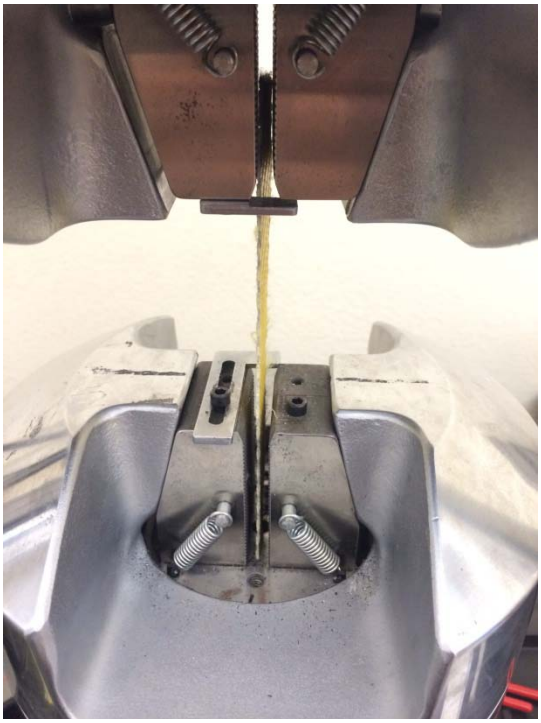

Figure 48: Test sample aligned in clamping jaws prior to being clamped into place.

Figure 49: Kevlar sample fully aligned and clamped into place before test.

The test samples were tested with a constant head speed of .0656 in/minute. The test parameters can be seen on the MTS Flextest screen below. The Maximum allowable elongation

was set to 10mm to keep the test machine from bottoming out. The test rate on Flextest in Figure 50 shows 0.1 in/minute because it can only display 1 decimal point. Once the parameters were set and all interlocks were off the test was begun.

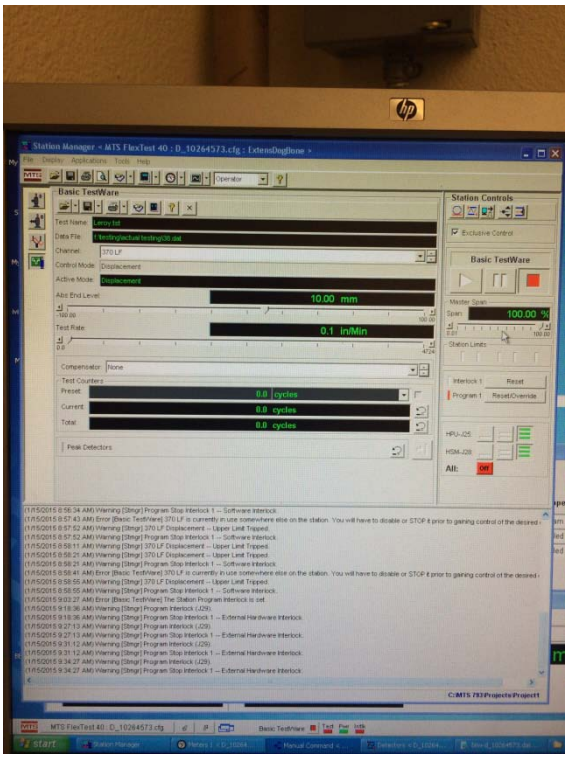


Figure 50: MTS Flextest test parameter setup.

The tests on average took 3 minutes from parameter setup and sample alignment to test start; it took under 1 minute to run the actual test until material failure. Once the material had failed the test was immediately stopped and the MTS heads were returned to the starting point and the sample examined. The examination included ensuring that the sample had not slipped in the gripping jaws and that the failure occurred within the test area. A failed sample still in the gripping jaws can be seen in figure 51.

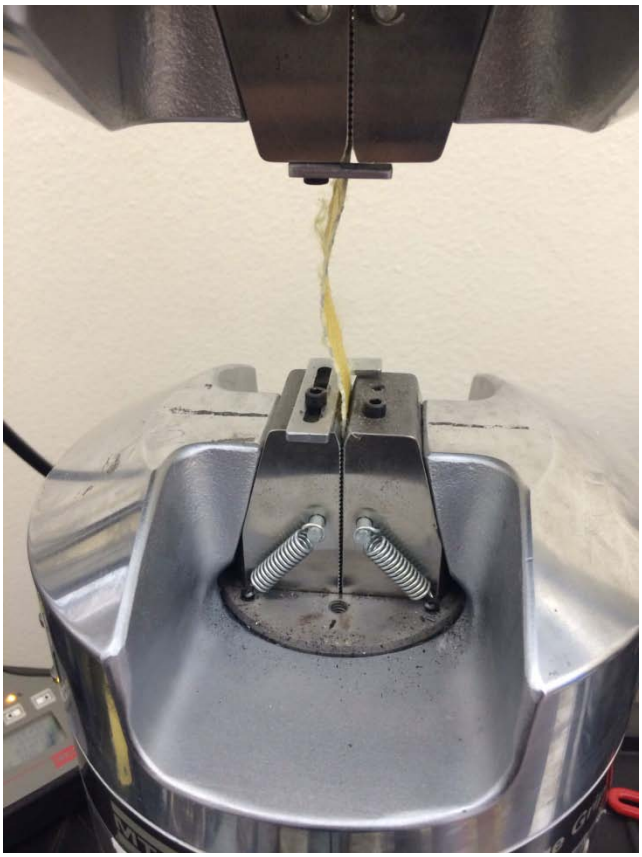

Figure 51: Test sample after being taken to failure and prior to being removed from gripping jaws.

Once the sample was removed from the jaws it was again inspected to ensure there was no slipping and to check the failure point of the Kevlar. Test sample 9 Rear can be seen in figure 52 showing uniform checkering on the grip area which demonstrates no jaw slipping and a failure in the center marked by the pen.

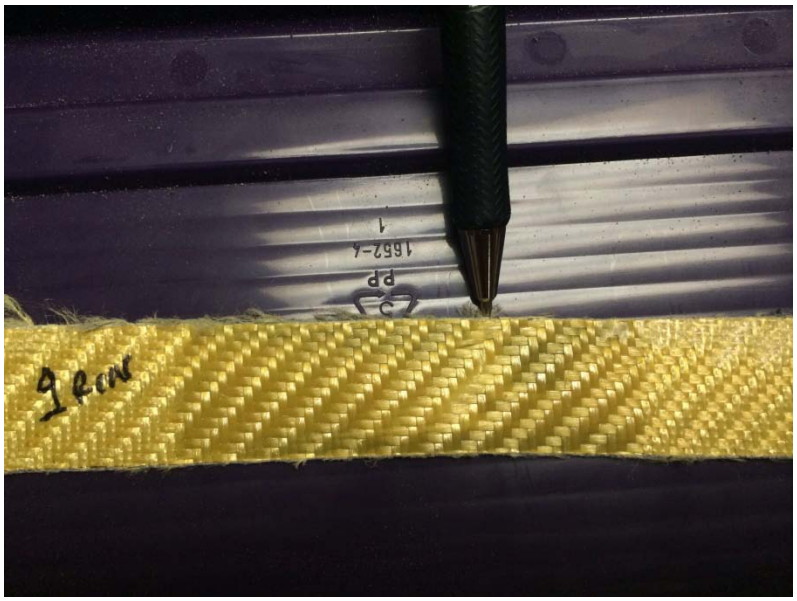


Figure 52: Test Sample 9Rear showing uniform checkering and a failure in the test area

All 55 test samples were all run through procedure and the pertinent data is listed in the results section as well as the appendix.

CHAPTER V

# 5. Results & Observations

## 5.1.MTS Tensile Testing

After each sample was tested its data file was loaded into a spreadsheet for analyzing. Each sample was looked at individually and as a set of each of its groups. The groupings are in type of composite or constituent material and radiation dose.

### 5.1.1. Material groupings

The first group of materials that was evaluated was the Kevlar/Poron/Kevlar group. This group was the basic material that all of the other materials were built upon and therefore was expected to perform as a baseline in this test. The control sample 1 does have a higher maximum stress level compared to the other samples which tells us that there was degradation on both faces of the composites that were exposed to radiation. As can be seen in Figure 53, the material degrades on the front face when exposed to higher levels of radiation but doesn't have a large drop off on any of the samples.

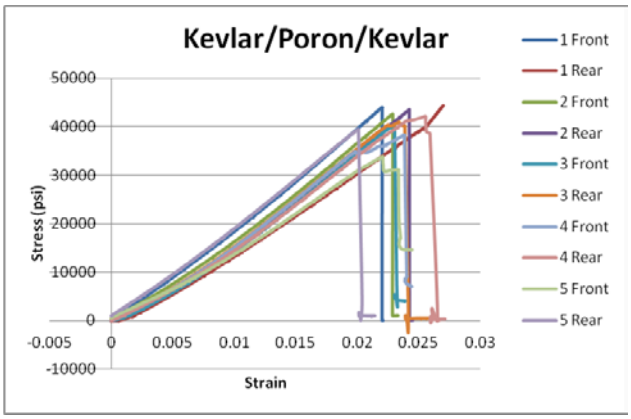


Figure 53: Tensile test results from the K?P?K composite

The Kevlar/Poron/H20/Kevlar composite shows more degradation on the front face of the Kevlar but does not show a drop in the rear Kevlar compared to the unexposed sample 6. This tells us that the added water within the samples has interacted with the gamma and attenuated some of its energy. The higher level of forward face degradation may be due to the energy passing through the front face twice once to enter and once to exit but this cannot be confirmed based on the data available. Figure 54 shows the stress strain relationship of the K/P/H/K composite.

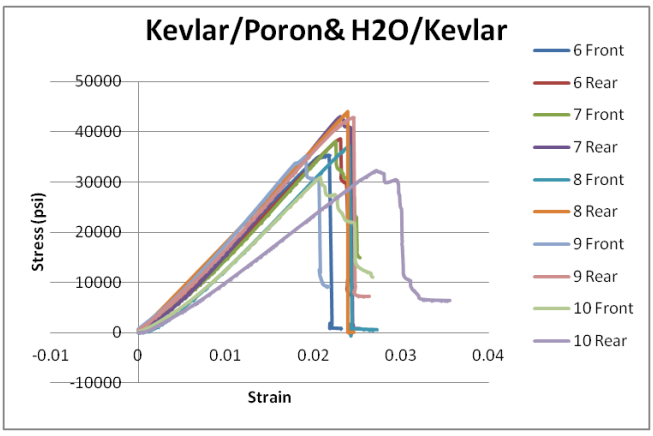


Figure 54: Stress Strain relationship of the K/P/H/K composite.

The Kevlar/Poron/Boron Nitride/Kevlar composite was one of the strongest performing in the SRIM testing and it performed well in the actual testing as well. Figure 55 shows this composite and its performance. In a similar fashion to the H2O composite, this grouping shows degradation on the front face that may be from double penetration of energy. This group has a much larger spread between the faces than the previous samples. The tensile strength of the rear face however, is seemingly unchanged.

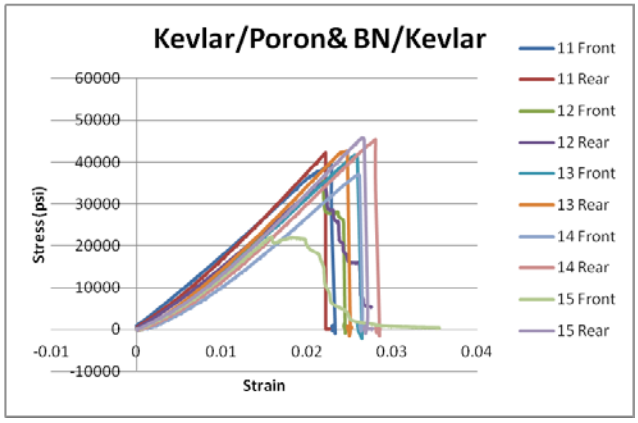


Figure 55: K/P/BN/K composite stress strain diagram.

The next series includes the chemical and moisture barrier Tyvek, while initially only added for its resistance to chemicals we can see that it has an added benefit of having extra mass in front of the radiation. This helped keep some of the energy off the front face of the Kevlar and we can in turn see an increase in tensile strength of the front Kevlar face compared to that of the two previous groups. While this composite did not have any liquid inside the Poron foam, it still kept the rear face relatively unchanged for many of the doses.

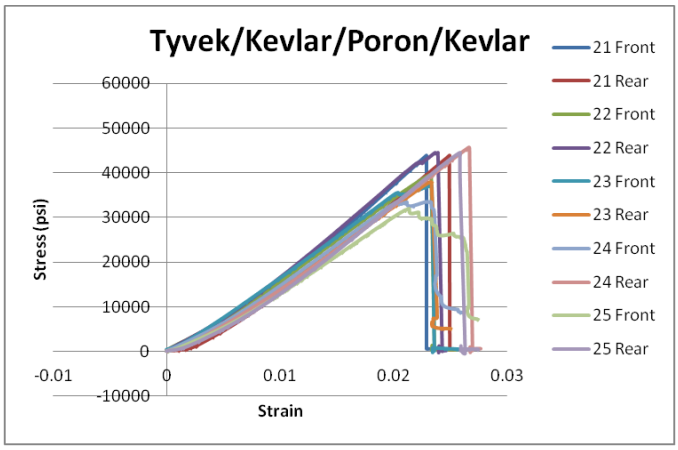


**Figure 56: T/K/P/K material stress strain diagram showing minimal rear face changes and lower face strength.**

The Tyvek/Kevlar/Poron/Boron Nitride/Kevlar material once again as a group shows greater face degradation than the same composite type without liquid inside. Since this phenomenon is in multiple samples we can assume that it is not a coincidence. The rear face of the composites is relatively unchanged with the sample that was at 500Gy being the exception. This material seems to have performed as one the best as far as rear face strength retention is concerned. This is backed up by the theoretical testing in SRIM and TRIM.

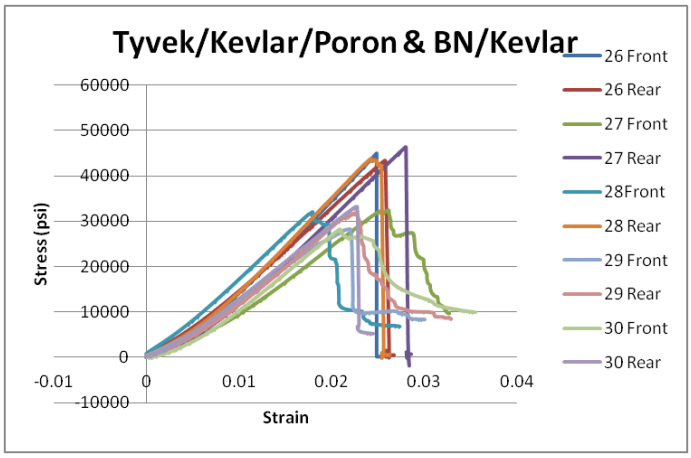


**Figure 57: T/K/BN/K Composite stress strain curves showing varying front and rear face strengths.**

The final grouping was that of just one face Kevlar material. This material was included as a baseline and so that interactions within the composite materials can be singled out as the

cause for shielding. As can be seen in figure 58, the Kevlar begins to gradually lose its strength based on the amount of radiation it has been exposed to . This relationship was expected at the outset of testing but seeing the numbers validate our expectations is a relief.

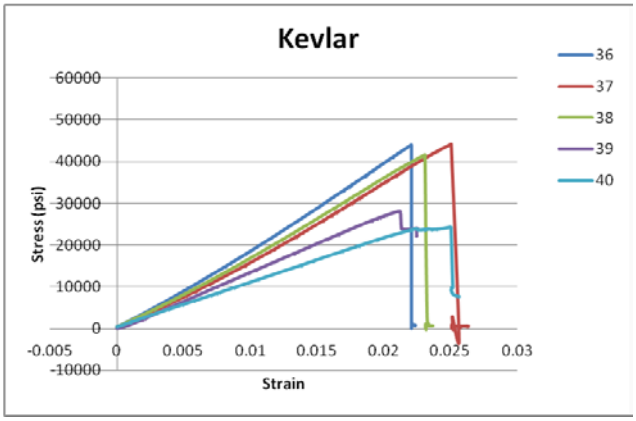


Figure 58: Kevlar skin stress strain showing degrading relationships based on their exposures

### 5.1.2. Radiation Groupings

The materials that were not exposed to any radiation show a variation in strain but have a very consistent stress relationship. This could be due to the different materials that interacted with the skins such as water, Boron Nitride or the glue used to attach the Tyvek to the Kevlar or it could just be variation due to material variation or testing setup. It was noted that a few of the samples had a slight curvature to them but conformed to ASTM D3039 as light finger pressure would allow them to return to a flat plane. The variation in strain could also be due to the machine having a minor distance to travel to take up the slack in the material during MTS testing.

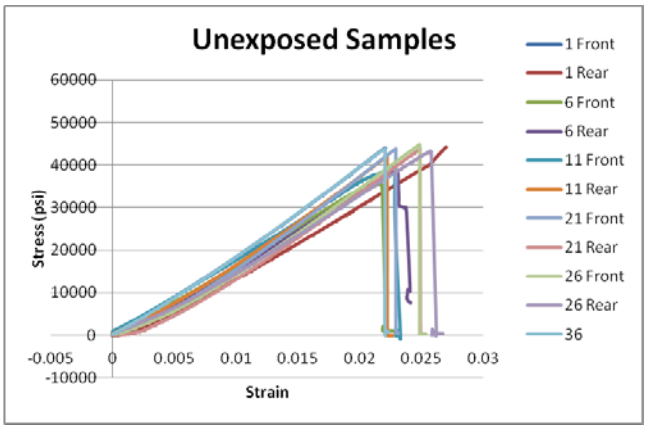


Figure 59: Comparison of all samples that were considered the control samples.

The first group that was exposed to radiation was exposed to the equivalent of a trip to Mars, a stay for approximately 1 year and the return voyage. The materials are first starting to show degradation in certain types. We can see that Sample 27 has a large drop in face strength even with this low dose. Other samples are also showing reduction of strength on their face sides but no noticeable changes are seen on the rear faces.

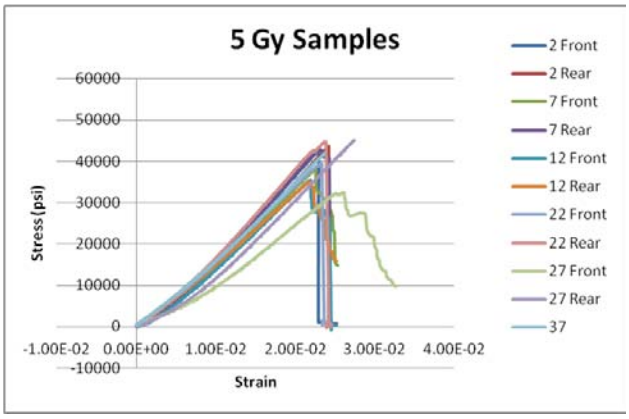


Figure 60: Samples exposed to 5Gy or the equivalent of one round trip voyage to Mars.

The 50 Gray test samples begin to show a slight degradation in rear face performance which can be expected due to the energy being passes through increasing by 10X. The samples continued to maintain their physical properties and strengths but the face values of multiple

samples began to fall to a lower strength level than that of the 5 Gy samples. Sample 27 shows greater face strength loss than its counterpart in the 5Gy group.

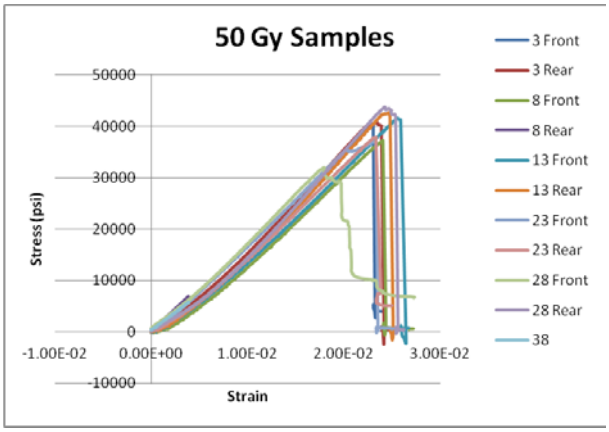


Figure 61: 50Gy exposure materials stress strain diagram

The 250 Gy exposed materials show a much larger variation in strength than do the other groups that have been exposed to radiation. This grouping has an average of 10ksi loss between the front face and the rear Kevlar face. The exceedingly high level of radiation that these samples have been exposed to does not seem to have much effect on the rear face while the front face is surely degrading.

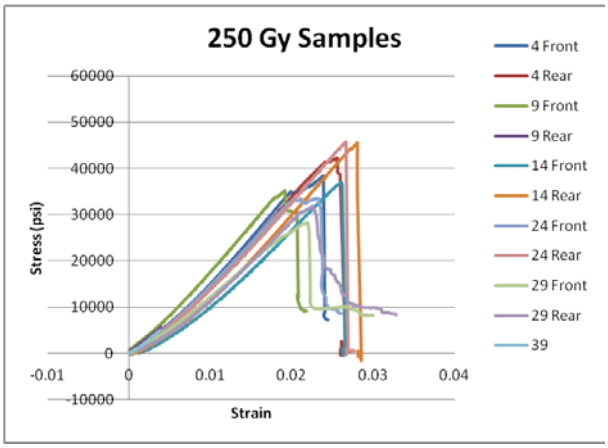


Figure 62: 250 Gy exposure samples showing loss in strength between the front and rear faces

The final group was the group that had the highest cumulative dose and was also exposed to multiple radiation cycles. This group shows the most degradation in the front and rear face as well as the greatest delta between the two faces. The level of radiation is 100X greater than the expected single mission dose. While this dose is exceedingly high we can use its data as validation that the materials will continue to keep their properties when exposed to this level of radiation energy. This directly correlates to lifespan in the space working environment.

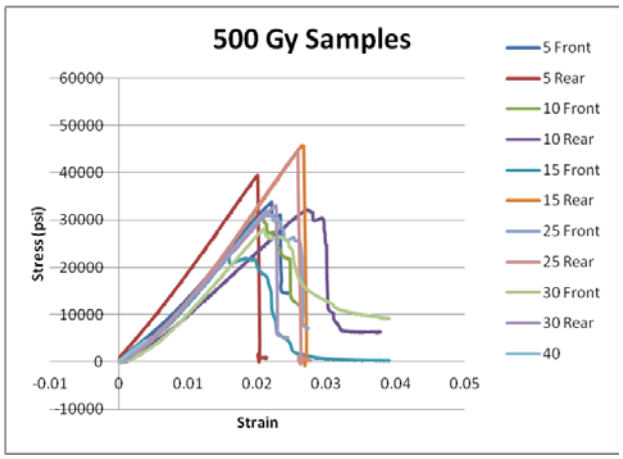


Figure 63: 500 Gy samples showing degradation but not completely losing material properties

### 5.1.3. Toughness

While maximum stress is a good indicator of the materials, it does not completely characterize the material. The toughness of the material is more telling as it takes into account the overall amount of energy the material is able to absorb before failure. For example in Figure 58, sample 36 & 37 both show a very similar stress level while sample 37 shows more ductility. This added ductility leads to additional area under the curve and therefore additional toughness

as can be verified in the toughness data in Table 5. We can see in Table 5 that for most cases the delta between face and rear pairs are generally positive. The few that are negative such as 5F/R is very close and is for the largest radiation dose. This material didn't have any interstitial material to reflect the gamma back. Looking at sample 10F/R we can see that there is a rather large delta between the front and rear face. This is most likely to the Poron/Water redirecting the energy back through the front face. This is seen with even greater delta in sample 15F/R which contained BN solution. The delta between the two samples is the greatest delta of any pair that was measured with the water sample being second. This helps validate our thoughts on the filled composite being able to shield at higher doses.

**Table 6: Toughness data for each Kevlar sample**

| Sample | | Toughness (Stress x Strain)(in·lbf | Delta Front to Rear | | Sample | | Toughness (Stress x Strain)(in·lbf·in–3)) | Delta Front to Rear |
|---|---|---|---|---|---|---|---|---|
| 1 | F | 1933298.924 | 838896.8049 | | 15 | F | 765433.8085 | 2090093.896 |
| 1 | R | 2772195.729 | | | 15 | R | 2855527.705 | |
| 2 | F | 1984055.813 | 266963.1656 | | 21 | F | 2000735.63 | 323223.873 |
| 2 | R | 2251018.979 | | | 21 | R | 2323959.503 | |
| 3 | F | 1866430.804 | 309070.5697 | | 22 | F | 1977557.787 | 356841.7917 |
| 3 | R | 2175501.374 | | | 22 | R | 2334399.579 | |
| 4 | F | 2103995.041 | 568566.1107 | | 23 | F | 1992340.215 | -143959.7561 |
| 4 | R | 2672561.151 | | | 23 | R | 1848380.459 | |
| 5 | F | 1495288.588 | -19255.63449 | | 24 | F | 1840210.111 | 1022411.911 |
| 5 | R | 1476032.954 | | | 24 | R | 2862622.023 | |
| 6 | F | 1638400.139 | 397041.2738 | | 25 | F | 2210241.452 | 384266.2441 |
| 6 | R | 2035441.413 | | | 25 | R | 2594507.696 | |
| 7 | F | 1727521.085 | 385710.5896 | | 26 | F | 2408423.862 | 196290.6443 |
| 7 | R | 2113231.674 | | | 26 | R | 2604714.506 | |
| 8 | F | 1902759.615 | 442321.3028 | | 27 | F | 1771642.169 | 1372018.007 |
| 8 | R | 2345080.918 | | | 27 | R | 3143660.175 | |
| 9 | F | 1215355.977 | 1232190.627 | | 28 | F | 1079620.865 | 1511824.67 |
| 9 | R | 2447546.604 | | | 28 | R | 2591445.534 | |
| 10 | F | 1180772.853 | 1195344.899 | | 29 | F | 1301838.595 | 190095.5125 |
| 10 | R | 2376117.752 | | | 29 | R | 1491934.108 | |
| 11 | F | 2000149.79 | -152214.2689 | | 30 | F | 1027239.932 | 524621.5821 |
| 11 | R | 1847935.522 | | | 30 | R | 1551861.514 | |
| 12 | F | 1510296.011 | 42139.0662 | | 36 | | 1946227.01 | |
| 12 | R | 1552435.077 | | | 37 | | 2523893.678 | |
| 13 | F | 2497907.507 | -157468.2699 | | 38 | | 2040942.502 | |
| 13 | R | 2340439.237 | | | 39 | | 1216049.19 | |
| 14 | F | 2187825.617 | 920286.3903 | | 40 | | 1565981.716 | |
| 14 | R | 3108112.007 | | | | | | |

CHAPTER VI

# 6. Conclusions

The testing can be seen as a positive step forward for the fluid filled composite materials world. However, more work and material characterization must be done before the material can be considered for widespread use. The results have shown that the material is able to survive in the desired operating environments and although not directly measured, its shielding properties are promising. Based on the strength of the rear face after exposure to varying levels of radiation compared to that of the front, we can see that while the basic materials do a sufficient job of attenuating gamma radiation, the composites with interstitial compounds perform marginally better. We can see that the materials all perform differently depending on the radiation dose they received but the Tyvek/Kevlar/Poron/Boron Nitride/Kevlar material seems to have performed better than the rest of the materials as far as rear face to front face strength delta. This is most likely due to the slight advantage in extra stopping mass the Tyvek gives to the composite compared to the identical material without Tyvek on the entry of the energy. This material also did a very good job in the toughness testing as its front face did not lose as much toughness as the same composite without Tyvek. It looks as though that the Tyvek has helped with the toughness and survivability of the front face. We can see that in general after exposure of over 250 Gy, many of the materials tested would not be suitable for use as their strength had fallen below 50% of the control group. The materials can be improved by adding different attenuating substances in the foam and ensuring that it is 100% full of compound.

# REFERENCES


[1]Phillips, L. et al, "Radiation Safety Manual" Stanford University. Retrieved from: http://web.stanford.edu/dept/EHS/prod/researchlab/radlaser/manual/rad_safety_manual.pdf

[2]USAF. "US Air Force Survival Handbook". Skyhorse Publishing 2008. ISBN - 9781602392458.

[3]WNA, World Nuclear Association, "What is Uranium? How does it work? http://www.world-nuclear.org/info/nuclear-fuel-cycle/introduction/what-is-uranium--how-does-it-work-/

[4]http://www.epa.gov/radiation/understand/protection_basics.html

[5] DuPont. "Personal Protection" http://www2.dupont.com/Personal_Protection/en_GB/assets/PDF/LIT_EN_NuclearIndustry.pdf

[6] Spillantini, P. Casolino M, Durante M, Mueller-Mellin R, Reitz G, Rossi L. "Shielding from cosmic radiation for interplanetary missions; active and passive methods.' Radiat Meas 42 (14-23) 2007.

[7] http://mars.jpl.nasa.gov/odyssey/mission/instruments/marie/

[8]Cucinotta, F. Kim, M. Chappel, L "Evaluating Shielding Approaches to Reduce Space radiation Cancer Risks" NASA Report NASATM-2012-217361, May 2012.

[9]Shavers, MR. Zapp N, Barber RE et al. "Implementation of ALARA radiation protection on the ISS through polyethylene shielding augmentation of the Service Module Crew Quarters." Advances in Space Research 34 (1333-1337) 2004.

[10] Lobascio, C. Briccarello, M et al. 'Accelerator Based Tests of Radiation Shielding Properties of Materials Used In Human Space Infrastructures.' Health Physics 94(3): 242-247; 2008

[11] Ghosh, AK. Morton B, Birbahadur N et al. "A Novel Material for an adaptive and stealth naval platform." Report N00014-09-M-0005 Office of Naval Research 2010

[12] Mathews, J. (2008). Shock and Vibration Characteristics of a Bio-Inspired Structure under Blast Loading MS Thesis, New Mexico Institute of Mining and Technology.

[13] Birbahadur, N. (2011 The High Strain-Rate Response of Polyurethane Foam and Kevlar composite. MS Thesis, New Mexico Institute of Mining and Technology.

[14]http://en.wikipedia.org/wiki/Boron_nitride

[15] Adams, Brent R. & Armstrong, RW et al. ASM Handbook Volume 10: Materials Characterization 9th Ed. American Society for Metals International, 1998.

[16] Ziegler, J.F. "The Stopping and Range of Ions in Matter", vol. 2-6, Pergamon Press, 1977-1985

[17] ASTM D3039

[18]http://en.wikipedia.org/wiki/Electronvolt

[19] http://marie.jsc.nasa.gov/Data/

[20]Macdonald, J. R. Ormrod, J. H. Duckworth, H. E. 'Stopping Cross Section in Boron of Low Atomic Number Atoms with Energies from 15 to 140 keV Z. Naturforschg. 21A, 130-34 (1966)

# 7. Appendices

## 7.1. Gamma Test Data

**Radiation Metrology Laboratory -- TLD Report**

This material should be treated as **OUO/ITAR** because it, when combined with performance information regarding the devices used in this test, may be ITAR (draft DOE guide, CG-MIC-1, sections 503.5, 505, 202, 303, 308.2). If this dosimetry information is never identified with the test object and its performance results, then this information would be **Unclassified - Unlimited Release**.

| | |
|---|---|
| Name | Leroy Garley |
| Org | NMT |
| Index | **517698** |
| ReadDate | 1/12/2015 |
| Email | |
| Project/Task | / |
| Facility | GIF-1 |
| Run No | 1183 |
| Start Date | 01/09/15 |
| Start Time | 09:20 |
| Stop Date | 01/09/15 |
| Stop Time | 09:21 |
| Reader | 03 |
| Batch | 35 |
| Num TLDs | 28 |
| Start Num | 1 |
| Comments | TLDs # 1-7 (4X) |

Note: The SI unit of radiation absorbed dose is the Gray (1 Gy = 100 Rads). At Co-60 energies, Dose(Si) = Dose(CaF2) x 1.02 Uncertainties are based on TLD response at Co-60 energies and are reported with a coverage factor of 1. Other uncertainties may exist depending on the radiation source or experimental configuration.

| Sequence | TLD | Time | Integral | Dose Gy(CaF2) | %UncA | %UncB | %UncTot |
|---|---|---|---|---|---|---|---|
| BKG | 01/BK | 10:21 | 309 | | | | |
| REF | 01/RF | 10:21 | 394502 | | | | |
| 1 | 01/01 | 10:22 | 6217346 | 7.529E+00 | 3.39 | 3.59 | 4.93 |
| 2 | 01/02 | 10:23 | 6328938 | 7.656E+00 | 3.39 | 3.59 | 4.93 |
| 3 | 01/03 | 10:24 | 6532594 | 7.889E+00 | 3.39 | 3.58 | 4.93 |
| 4 | 01/04 | 10:24 | 6537889 | 7.895E+00 | 3.39 | 3.58 | 4.93 |
| 5 | 01/05 | 10:25 | 6469405 | 7.817E+00 | 3.39 | 3.58 | 4.93 |
| 6 | 01/06 | 10:26 | 6236234 | 7.550E+00 | 3.39 | 3.59 | 4.93 |
| 7 | 01/07 | 10:27 | 6250563 | 7.567E+00 | 3.39 | 3.59 | 4.93 |
| 8 | 01/08 | 10:27 | 6366073 | 7.699E+00 | 3.39 | 3.58 | 4.93 |
| 9 | 01/09 | 10:28 | 6394986 | 7.732E+00 | 3.39 | 3.58 | 4.93 |
| 10 | 01/10 | 10:29 | 6083502 | 7.375E+00 | 3.39 | 3.59 | 4.93 |
| 11 | 01/11 | 10:29 | 6327589 | 7.655E+00 | 3.39 | 3.59 | 4.93 |
| 12 | 01/12 | 10:30 | 6113227 | 7.409E+00 | 3.39 | 3.59 | 4.93 |
| 13 | 01/13 | 10:31 | 6007816 | 7.288E+00 | 3.39 | 3.59 | 4.93 |
| 14 | 01/14 | 10:32 | 6443386 | 7.788E+00 | 3.39 | 3.58 | 4.93 |
| 15 | 01/15 | 10:32 | 6092849 | 7.386E+00 | 3.39 | 3.59 | 4.93 |
| 16 | 01/16 | 10:33 | 6382533 | 7.718E+00 | 3.39 | 3.58 | 4.93 |
| 17 | 01/17 | 10:34 | 6471618 | 7.820E+00 | 3.39 | 3.58 | 4.93 |
| 18 | 01/18 | 10:34 | 6530607 | 7.887E+00 | 3.39 | 3.58 | 4.93 |

## Radiation Metrology Laboratory -- TLD Report

This material should be treated as **OUO/ITAR** because it, when combined with performance information regarding the devices used in this test, may be ITAR (draft DOE guide, CG-MIC-1, sections 503.5, 505, 202, 303, 308.2). If this dosimetry information is never identified with the test object and its performance results, then this information would be **Undassified - Unlimited Release**.

| | |
|---|---|
| Name | Leroy Garley |
| Org | NMT |
| Index | **517699** |
| ReadDate | 1/12/2015 |
| Email | |
| Project/Task | / |
| Facility | GIF-1 |
| Run No | 1184 |
| Start Date | 01/09/15 |
| Start Time | 09:58 |
| Stop Date | 01/09/15 |
| Stop Time | 10:06 |
| Reader | 03 |
| Batch | 35 |
| Num TLDs | 12 |
| Start Num | 1 |
| Comments | TLDs # 1-3 (4X) |

Note: The SI unit of radiation absorbed dose is the Gray (1 Gy = 100 Rads). At Co-60 energies, Dose(Si) = Dose(CaF2) x 1.02 Uncertainties are based on TLD response at Co-60 energies and are reported with a coverage factor of 1. Other uncertainties may exist depending on the radiation source or experimental configuration.

| Sequence | TLD | Time | Integral | Dose Gy(CaF2) | %UncA | %UncB | %UncTot |
|---|---|---|---|---|---|---|---|
| BKG | 01/BK | 10:47 | 310 | | | | |
| REF | 01/RF | 10:48 | 396679 | | | | |
| 1 | 01/01 | 10:48 | 61320577 | 6.093E+01 | 2.57 | 4.62 | 5.29 |
| 2 | 01/02 | 10:49 | 57945910 | 5.786E+01 | 2.57 | 4.62 | 5.29 |
| 3 | 01/03 | 10:50 | 58979828 | 5.880E+01 | 2.57 | 4.62 | 5.29 |
| 4 | 01/04 | 10:50 | 62125864 | 6.166E+01 | 2.57 | 4.62 | 5.29 |
| 5 | 01/05 | 10:51 | 57012903 | 5.701E+01 | 2.57 | 4.62 | 5.29 |
| 6 | 01/06 | 10:52 | 58576427 | 5.844E+01 | 2.57 | 4.62 | 5.29 |
| 7 | 01/07 | 10:53 | 57004829 | 5.700E+01 | 2.57 | 4.62 | 5.29 |
| 8 | 01/08 | 10:53 | 54173854 | 5.441E+01 | 2.56 | 4.62 | 5.29 |
| 9 | 01/09 | 10:54 | 58030222 | 5.794E+01 | 2.57 | 4.62 | 5.29 |
| 10 | 01/10 | 10:55 | 59789248 | 5.954E+01 | 2.57 | 4.62 | 5.29 |
| 11 | 01/11 | 10:56 | 58591351 | 5.845E+01 | 2.57 | 4.62 | 5.29 |
| 12 | 01/12 | 10:56 | 59996622 | 5.973E+01 | 2.57 | 4.62 | 5.29 |

## Radiation Metrology Laboratory -- TLD Report

This material should be treated as **OUO/ITAR** because it, when combined with performance information regarding the devices used in this test, may be ITAR (draft DOE guide, CG-MIC-1, sections 503.5, 505, 202, 303, 308.2). If this dosimetry information is never identified with the test object and its performance results, then this information would be **Undassified - Unlimited Release**.

| | |
|---|---|
| Name | Leroy Garley |
| Org | NMT |
| Index | **517701** |
| ReadDate | 1/12/2015 |
| Email | |
| Project/Task | / |
| Facility | GIF-1 |
| Run No | 1185 |
| Start Date | 01/09/15 |
| Start Time | 10:37 |
| Stop Date | 01/09/15 |
| Stop Time | 11:19 |
| Reader | 03 |
| Batch | 35 |
| Num TLDs | 12 |
| Start Num | 1 |
| Comments | TLDs # 1-3 (4X) |

Note: The SI unit of radiation absorbed dose is the Gray (1 Gy = 100 Rads). At Co-60 energies, Dose(Si) = Dose(CaF2) x 1.02 Uncertainties are based on TLD response at Co-60 energies and are reported with a coverage factor of 1. Other uncertainties may exist depending on the radiation source or experimental configuration.

| Sequence | TLD | Time | Integral | Dose Gy(CaF2) | %UncA | %UncB | %UncTot |
|---|---|---|---|---|---|---|---|
| BKG | 01/BK | 10:59 | 307 | | | | |
| REF | 01/RF | 10:59 | 396209 | | | | |
| 1 | 01/01 | 11:00 | 302930689 | 2.615E+02 | 3.52 | 3.66 | 5.08 |
| 2 | 01/02 | 11:01 | 320766448 | 2.769E+02 | 3.51 | 3.67 | 5.08 |
| 3 | 01/03 | 11:01 | 305692379 | 2.639E+02 | 3.51 | 3.66 | 5.08 |
| 4 | 01/04 | 11:02 | 317178563 | 2.738E+02 | 3.51 | 3.67 | 5.08 |
| 5 | 01/05 | 11:03 | 306753714 | 2.648E+02 | 3.51 | 3.66 | 5.08 |
| 6 | 01/06 | 11:04 | 313758998 | 2.708E+02 | 3.51 | 3.67 | 5.08 |
| 7 | 01/07 | 11:04 | 309163641 | 2.669E+02 | 3.51 | 3.66 | 5.08 |
| 8 | 01/08 | 11:05 | 316543876 | 2.732E+02 | 3.51 | 3.67 | 5.08 |
| 9 | 01/09 | 11:06 | 315818714 | 2.726E+02 | 3.51 | 3.67 | 5.08 |
| 10 | 01/10 | 11:07 | 300706125 | 2.596E+02 | 3.52 | 3.66 | 5.08 |
| 11 | 01/11 | 11:07 | 303289184 | 2.619E+02 | 3.52 | 3.66 | 5.08 |
| 12 | 01/12 | 11:08 | 300584398 | 2.595E+02 | 3.52 | 3.66 | 5.08 |

## Radiation Metrology Laboratory -- TLD Report

This material should be treated as **OUO/ITAR** because it, when combined with performance information regarding the devices used in this test, may be ITAR (draft DOE guide, CG-MIC-1, sections 503.5, 505, 202, 303, 308.2). If this dosimetry information is never identified with the test object and its performance results, then this information would be **Unclassified - Unlimited Release**.

| | |
|---|---|
| Name | Leroy Garley |
| Org | NMT |
| Index | **517702** |
| ReadDate | 1/12/2015 |
| Email | |
| Project/Task | / |
| Facility | GIF-1 |
| Run No | 1186 |
| Start Date | 01/09/15 |
| Start Time | 11:42 |
| Stop Date | 01/09/15 |
| Stop Time | 12:14 |
| Reader | 03 |
| Batch | 35 |
| Num TLDs | 12 |
| Start Num | 1 |
| Comments | TLDs # 1-3 (4X) |

Note: The SI unit of radiation absorbed dose is the Gray (1 Gy = 100 Rads). At Co-60 energies, Dose(Si) = Dose(CaF2) x 1.02 Uncertainties are based on TLD response at Co-60 energies and are reported with a coverage factor of 1. Other uncertainties may exist depending on the radiation source or experimental configuration.

| Sequence | TLD | Time | Integral | Dose Gy(CaF2) | %UncA | %UncB | %UncTot |
|---|---|---|---|---|---|---|---|
| BKG | 01/BK | 11:39 | 343 | | | | |
| REF | 01/RF | 11:40 | 396194 | | | | |
| 1 | 01/01 | 11:40 | 257801957 | 2.231E+02 | 3.52 | 3.64 | 5.06 |
| 2 | 01/02 | 11:41 | 225500086 | 1.995E+02 | 2.67 | 4.17 | 4.95 |
| 3 | 01/03 | 11:42 | 252127292 | 2.183E+02 | 3.52 | 3.63 | 5.06 |
| 4 | 01/04 | 11:43 | 247243925 | 2.142E+02 | 3.51 | 3.63 | 5.05 |
| 5 | 01/05 | 11:43 | 265620076 | 2.297E+02 | 3.52 | 3.64 | 5.06 |
| 6 | 01/06 | 11:44 | 264046149 | 2.284E+02 | 3.52 | 3.64 | 5.06 |
| 7 | 01/07 | 11:45 | 271457908 | 2.347E+02 | 3.52 | 3.64 | 5.07 |
| 8 | 01/08 | 11:45 | 251902264 | 2.181E+02 | 3.52 | 3.63 | 5.06 |
| 9 | 01/09 | 11:46 | 261303429 | 2.261E+02 | 3.52 | 3.64 | 5.06 |
| 10 | 01/10 | 11:47 | 260452430 | 2.254E+02 | 3.52 | 3.64 | 5.06 |
| 11 | 01/11 | 11:48 | 280811526 | 2.426E+02 | 3.52 | 3.65 | 5.07 |
| 12 | 01/12 | 11:48 | 265891242 | 2.300E+02 | 3.52 | 3.64 | 5.06 |

## 7.2. MTS Sample Test Data Sheet

Each data sheet is over 200 pages long so only a selection of the first sample is shown.

MTS793|BTW|ENU|1|2|.|/|:|1|0|0|A

| | | | | | | | |
|---|---|---|---|---|---|---|---|
| Data Header: | | Sample1Front | | | | Time: | 20.022461 |
| Data Acqui Timed | | | | | | | |
| Station Nar | D_10264573.cfg | | | | | | 0.022 |
| Test File Na | Leroy.tst | | | | | | 16.129 |
| 370 LF Disp | 370 LF Forc | 370 LF Stra | Time | | | | 0.000016129 |
| mm | kN | % | Sec | inches of elongation | lbs | stress (psi) | strain |
| 0.001155 | 0.030076 | 0.148318 | 0.026367 | 4.54612E-05 | 6.761433 | 307.3379 | 1.51537E-05 |
| 0.000167 | 0.030284 | 1.10387 | 0.036133 | 6.58704E-06 | 6.808212 | 309.4642 | 2.19568E-06 |
| 0.000303 | 0.030326 | 0.78095 | 0.045898 | 1.19132E-05 | 6.817597 | 309.8908 | 3.97108E-06 |
| -0.00055 | 0.028552 | 0.471908 | 0.055664 | -2.18445E-05 | 6.418853 | 291.766 | -7.2815E-06 |
| -0.00132 | 0.030559 | 0.832737 | 0.06543 | -5.20879E-05 | 6.86996 | 312.2709 | -1.7363E-05 |
| -0.00051 | 0.029847 | -1.24918 | 0.075195 | -2.00997E-05 | 6.709766 | 304.9894 | -6.6999E-06 |
| -0.00116 | 0.029918 | 1.365041 | 0.084961 | -4.55121E-05 | 6.725725 | 305.7148 | -1.5171E-05 |
| 0.00045 | 0.031862 | 0.316043 | 0.094727 | 1.76977E-05 | 7.162836 | 325.5835 | 5.89922E-06 |
| 0.001143 | 0.031421 | 0.755868 | 0.104492 | 4.50053E-05 | 7.063611 | 321.0732 | 1.50018E-05 |
| -0.0004 | 0.032683 | -1.20246 | 0.114258 | -1.59021E-05 | 7.347532 | 333.9787 | -5.3007E-06 |
| 0.000463 | 0.03165 | 1.208558 | 0.124023 | 1.82445E-05 | 7.115263 | 323.421 | 6.08149E-06 |
| 0.001134 | 0.032904 | 0.339042 | 0.133789 | 4.4644E-05 | 7.397011 | 336.2278 | 1.48813E-05 |
| 0.001747 | 0.033128 | 0.626561 | 0.143555 | 6.87775E-05 | 7.447443 | 338.5202 | 2.29258E-05 |
| 0.000982 | 0.033839 | 0.158982 | 0.15332 | 3.8654E-05 | 7.607381 | 345.79 | 1.28847E-05 |
| 0.003175 | 0.035067 | 1.116502 | 0.163086 | 0.000125018 | 7.883319 | 358.3327 | 4.16726E-05 |
| 0.002239 | 0.036026 | 0.792418 | 0.172852 | 8.81567E-05 | 8.098912 | 368.1324 | 2.93856E-05 |
| 0.003345 | 0.037304 | 0.489847 | 0.182617 | 0.00013169 | 8.386236 | 381.1925 | 4.38966E-05 |
| 0.00322 | 0.038864 | 0.853018 | 0.192383 | 0.000126787 | 8.737035 | 397.1379 | 4.22625E-05 |
| 0.004131 | 0.03955 | -1.22147 | 0.202148 | 0.000162654 | 8.89125 | 404.1477 | 5.42179E-05 |
| 0.004094 | 0.038994 | 1.385821 | 0.211914 | 0.000161188 | 8.766189 | 398.4631 | 5.37294E-05 |
| 0.003958 | 0.039062 | 0.338176 | 0.22168 | 0.000155838 | 8.781515 | 399.1598 | 5.1946E-05 |
| 0.004392 | 0.04019 | 0.790605 | 0.231445 | 0.000172929 | 9.03514 | 410.6882 | 5.76429E-05 |
| 0.004805 | 0.040891 | -1.21059 | 0.241211 | 0.000189155 | 9.192707 | 417.8503 | 6.30515E-05 |
| 0.005516 | 0.041351 | 1.23926 | 0.250977 | 0.000217178 | 9.296103 | 422.5502 | 7.23926E-05 |
| 0.00571 | 0.041019 | 0.334206 | 0.260742 | 0.000224802 | 9.22151 | 419.1595 | 7.49339E-05 |
| 0.005713 | 0.04266 | 0.624965 | 0.270508 | 0.000224926 | 9.590315 | 435.9234 | 7.49754E-05 |
| 0.006237 | 0.044466 | 0.168468 | 0.280273 | 0.000245536 | 9.996387 | 454.3812 | 8.18455E-05 |
| 0.005011 | 0.043446 | 1.105952 | 0.290039 | 0.000197265 | 9.767038 | 443.9563 | 6.57551E-05 |
| 0.006193 | 0.044324 | 0.803216 | 0.299805 | 0.000243815 | 9.964395 | 452.9271 | 8.12715E-05 |
| 0.006804 | 0.045942 | 0.495599 | 0.30957 | 0.000267873 | 10.32815 | 469.4615 | 8.92911E-05 |
| 0.007954 | 0.046529 | 0.859362 | 0.319336 | 0.000313148 | 10.46017 | 475.4624 | 0.000104383 |
| 0.007462 | 0.045792 | -1.23439 | 0.329102 | 0.000293765 | 10.29442 | 467.9282 | 9.79217E-05 |
| 0.007739 | 0.046707 | 1.381438 | 0.338867 | 0.000304669 | 10.5002 | 477.2818 | 0.000101556 |
| 0.008814 | 0.047186 | 0.330911 | 0.348633 | 0.000347005 | 10.60782 | 482.1736 | 0.000115668 |
| 0.007556 | 0.047803 | 0.774819 | 0.358398 | 0.000297492 | 10.74647 | 488.4761 | 9.9164E-05 |
| 0.00831 | 0.047267 | -1.1665 | 0.368164 | 0.000327147 | 10.62598 | 482.999 | 0.000109049 |
| 0.008603 | 0.049103 | 1.238511 | 0.37793 | 0.000338684 | 11.03884 | 501.7656 | 0.000112895 |
| 0.008356 | 0.047567 | 0.322761 | 0.387695 | 0.000328993 | 10.69345 | 486.066 | 0.000109664 |
| 0.009664 | 0.048779 | 0.639329 | 0.397461 | 0.000380467 | 10.96604 | 498.4562 | 0.000126822 |

| | | | | | | | |
|---|---|---|---|---|---|---|---|
| 0.009831 | 0.049995 | 0.174805 | 0.407227 | 0.000387031 | 11.23934 | 510.8789 | 0.00012901 |
| 0.007853 | 0.049973 | 1.129911 | 0.416992 | 0.000309165 | 11.23437 | 510.6532 | 0.000103055 |
| 0.009419 | 0.050409 | 0.814278 | 0.426758 | 0.000370816 | 11.33231 | 515.1048 | 0.000123605 |
| 0.008915 | 0.049918 | 0.493694 | 0.436523 | 0.000350969 | 11.22197 | 510.0895 | 0.00011699 |
| 0.009881 | 0.052298 | 0.860145 | 0.446289 | 0.000389028 | 11.75717 | 534.4166 | 0.000129676 |
| 0.009659 | 0.051639 | -1.24313 | 0.456055 | 0.000380295 | 11.60885 | 527.6751 | 0.000126765 |
| 0.010776 | 0.051528 | 1.359363 | 0.46582 | 0.000424233 | 11.58387 | 526.5395 | 0.000141411 |
| 0.011978 | 0.053002 | 0.318175 | 0.475586 | 0.000471561 | 11.91543 | 541.6106 | 0.000157187 |
| 0.011041 | 0.053114 | 0.751803 | 0.485352 | 0.000434675 | 11.94054 | 542.7516 | 0.000144892 |
| 0.01205 | 0.054726 | -1.18777 | 0.495117 | 0.000474427 | 12.30296 | 559.2255 | 0.000158142 |
| 0.012158 | 0.055624 | 1.237375 | 0.504883 | 0.000478661 | 12.50485 | 568.4023 | 0.000159554 |
| 0.012693 | 0.055807 | 0.356542 | 0.514648 | 0.00049973 | 12.54595 | 570.2707 | 0.000166577 |
| 0.012471 | 0.056352 | 0.635063 | 0.524414 | 0.000490997 | 12.6684 | 575.8365 | 0.000163666 |
| 0.012593 | 0.054763 | 0.170951 | 0.53418 | 0.000495801 | 12.31127 | 559.6033 | 0.000165267 |
| 0.013007 | 0.057389 | 1.133478 | 0.543945 | 0.000512105 | 12.90161 | 586.4368 | 0.000170702 |
| 0.013987 | 0.058077 | 0.806849 | 0.553711 | 0.00055068 | 13.05611 | 593.4597 | 0.00018356 |
| 0.014679 | 0.060556 | 0.504332 | 0.563477 | 0.000577927 | 13.61351 | 618.7961 | 0.000192642 |
| 0.012952 | 0.059122 | 0.852321 | 0.573242 | 0.000509917 | 13.29125 | 604.1478 | 0.000169972 |
| 0.014534 | 0.059907 | -1.24369 | 0.583008 | 0.0005722 | 13.46772 | 612.1693 | 0.000190733 |
| 0.015494 | 0.060542 | 1.359285 | 0.592773 | 0.000610011 | 13.61027 | 618.6486 | 0.000203337 |
| 0.015461 | 0.061805 | 0.338658 | 0.602539 | 0.000608687 | 13.89436 | 631.5619 | 0.000202896 |
| 0.014243 | 0.061952 | 0.794294 | 0.612305 | 0.000560752 | 13.9273 | 633.0591 | 0.000186917 |
| 0.016089 | 0.062885 | -1.18012 | 0.62207 | 0.00063343 | 14.13709 | 642.5952 | 0.000211143 |
| 0.016083 | 0.061979 | 1.248816 | 0.631836 | 0.000633198 | 13.93337 | 633.3351 | 0.000211066 |
| 0.015589 | 0.062806 | 0.358637 | 0.641602 | 0.000613746 | 14.11941 | 641.7915 | 0.000204582 |
| 0.015768 | 0.064615 | 0.633391 | 0.651367 | 0.00062079 | 14.52599 | 660.2722 | 0.00020693 |
| 0.016268 | 0.06475 | 0.133971 | 0.661133 | 0.000640458 | 14.55643 | 661.6558 | 0.000213486 |
| 0.017541 | 0.065053 | 1.110399 | 0.670898 | 0.000690573 | 14.6245 | 664.7501 | 0.000230191 |
| 0.017607 | 0.066399 | 0.791203 | 0.680664 | 0.000693206 | 14.92712 | 678.5057 | 0.000231069 |
| 0.01609 | 0.066345 | 0.487418 | 0.69043 | 0.000633471 | 14.91496 | 677.9528 | 0.000211157 |
| 0.016924 | 0.066322 | 0.844375 | 0.700195 | 0.000666316 | 14.90979 | 677.7177 | 0.000222105 |
| 0.017644 | 0.068641 | -1.22754 | 0.709961 | 0.000694636 | 15.43109 | 701.4131 | 0.000231545 |
| 0.018537 | 0.067269 | 1.363378 | 0.719727 | 0.000729812 | 15.12273 | 687.3968 | 0.000243271 |
| 0.018522 | 0.067983 | 0.327963 | 0.729492 | 0.000729196 | 15.28313 | 694.6876 | 0.000243065 |
| 0.017915 | 0.068993 | 0.780735 | 0.739258 | 0.000705307 | 15.51031 | 705.0143 | 0.000235102 |
| 0.017688 | 0.069041 | -1.18494 | 0.749023 | 0.000696395 | 15.52098 | 705.4991 | 0.000232132 |
| 0.018837 | 0.069484 | 1.232158 | 0.758789 | 0.000741622 | 15.62054 | 710.0244 | 0.000247207 |
| 0.018969 | 0.06961 | 0.333674 | 0.768555 | 0.000746811 | 15.64901 | 711.3187 | 0.000248937 |
| 0.018891 | 0.072462 | 0.652004 | 0.77832 | 0.000743747 | 16.29 | 740.4543 | 0.000247916 |
| 0.019402 | 0.072892 | 0.165743 | 0.788086 | 0.000763843 | 16.3868 | 744.8544 | 0.000254614 |
| 0.020129 | 0.072417 | 1.107674 | 0.797852 | 0.000792483 | 16.28004 | 740.0019 | 0.000264161 |
| 0.019095 | 0.073294 | 0.817553 | 0.807617 | 0.000751766 | 16.47714 | 748.9609 | 0.000250589 |
| 0.020844 | 0.074508 | 0.481028 | 0.817383 | 0.000820644 | 16.75016 | 761.3708 | 0.000273548 |
| 0.021357 | 0.074873 | 0.837104 | 0.827148 | 0.000840819 | 16.83214 | 765.0971 | 0.000280273 |
| 0.021513 | 0.076391 | -1.23679 | 0.836914 | 0.000846971 | 17.17335 | 780.6067 | 0.000282324 |
| 0.020848 | 0.075477 | 1.375973 | 0.84668 | 0.000820794 | 16.96798 | 771.2716 | 0.000273598 |
| 0.021138 | 0.0776 | 0.334472 | 0.856445 | 0.000832188 | 17.44525 | 792.9661 | 0.000277396 |

| | | | | | | | |
|---|---|---|---|---|---|---|---|
| 0.022877 | 0.076777 | 0.747788 | 0.866211 | 0.000900654 | 17.26005 | 784.5476 | 0.000300218 |
| 0.022888 | 0.077869 | -1.19179 | 0.875977 | 0.000901102 | 17.50556 | 795.7074 | 0.000300367 |
| 0.023297 | 0.079639 | 1.226945 | 0.885742 | 0.000917208 | 17.90354 | 813.7975 | 0.000305736 |
| 0.02235 | 0.078558 | 0.307238 | 0.895508 | 0.000879905 | 17.66054 | 802.7518 | 0.000293302 |
| 0.024991 | 0.079278 | 0.608574 | 0.905273 | 0.000983894 | 17.82244 | 810.1107 | 0.000327965 |
| 0.023883 | 0.079569 | 0.169082 | 0.915039 | 0.000940285 | 17.88786 | 813.0847 | 0.000313428 |
| 0.025111 | 0.081098 | 1.108008 | 0.924805 | 0.00098863 | 18.23145 | 828.7022 | 0.000329543 |
| 0.024639 | 0.080749 | 0.766271 | 0.93457 | 0.000970034 | 18.15318 | 825.1443 | 0.000323345 |
| 0.024394 | 0.081498 | 0.4741 | 0.944336 | 0.000960396 | 18.32156 | 832.7983 | 0.000320132 |
| 0.024561 | 0.082846 | 0.817837 | 0.954102 | 0.000966951 | 18.62453 | 846.5695 | 0.000322317 |
| 0.0256 | 0.081678 | -1.26284 | 0.963867 | 0.001007863 | 18.36205 | 834.6388 | 0.000335954 |
| 0.024359 | 0.08188 | 1.369411 | 0.973633 | 0.000958999 | 18.40735 | 836.6977 | 0.000319666 |
| 0.025787 | 0.083385 | 0.323094 | 0.983398 | 0.001015247 | 18.7458 | 852.0817 | 0.000338416 |
| 0.02541 | 0.084533 | 0.766581 | 0.993164 | 0.001000399 | 19.00383 | 863.8106 | 0.000333466 |
| 0.026495 | 0.084387 | -1.18623 | 1.00293 | 0.001043098 | 18.97088 | 862.3127 | 0.000347699 |
| 0.025583 | 0.08584 | 1.224213 | 1.012695 | 0.001007214 | 19.29767 | 877.167 | 0.000335738 |
| 0.027161 | 0.086056 | 0.308468 | 1.022461 | 0.001069322 | 19.34605 | 879.3659 | 0.000356441 |
| 0.027098 | 0.086315 | 0.605861 | 1.032227 | 0.001066855 | 19.40439 | 882.0177 | 0.000355618 |
| 0.027313 | 0.086977 | 0.175316 | 1.041992 | 0.001075312 | 19.55323 | 888.7832 | 0.000358437 |
| 0.026862 | 0.086594 | 1.11752 | 1.051758 | 0.001057576 | 19.46718 | 884.8718 | 0.000352525 |
| 0.026634 | 0.088239 | 0.775214 | 1.061523 | 0.001048567 | 19.83692 | 901.678 | 0.000349522 |
| 0.027239 | 0.088571 | 0.468874 | 1.071289 | 0.001072397 | 19.91155 | 905.0702 | 0.000357466 |
| 0.027338 | 0.090017 | 0.819509 | 1.081055 | 0.001076302 | 20.23672 | 919.8508 | 0.000358767 |
| 0.02801 | 0.090322 | -1.25736 | 1.09082 | 0.00110274 | 20.30511 | 922.9595 | 0.00036758 |
| 0.027326 | 0.090818 | 1.353285 | 1.100586 | 0.001075835 | 20.41673 | 928.0334 | 0.000358612 |
| 0.029241 | 0.090732 | 0.297593 | 1.110352 | 0.001151224 | 20.39746 | 927.1573 | 0.000383741 |
| 0.028835 | 0.092421 | 0.766108 | 1.120117 | 0.001135229 | 20.77708 | 944.4127 | 0.00037841 |
| 0.028613 | 0.09347 | -1.20482 | 1.129883 | 0.001126506 | 21.01298 | 955.1353 | 0.000375502 |
| 0.030583 | 0.093907 | 1.242483 | 1.139648 | 0.001204064 | 21.11113 | 959.5968 | 0.000401355 |
| 0.030259 | 0.093717 | 0.342279 | 1.149414 | 0.001191284 | 21.06841 | 957.6549 | 0.000397095 |
| 0.028915 | 0.094589 | 0.620696 | 1.15918 | 0.001138389 | 21.26446 | 966.5664 | 0.000379463 |
| 0.029854 | 0.095428 | 0.147605 | 1.168945 | 0.001175353 | 21.4531 | 975.141 | 0.000391784 |
| 0.030809 | 0.094986 | 1.094304 | 1.178711 | 0.001212958 | 21.3536 | 970.6181 | 0.000404319 |
| 0.03138 | 0.096509 | 0.793391 | 1.188477 | 0.001235443 | 21.69602 | 986.1829 | 0.000411814 |
| 0.031026 | 0.096552 | 0.481652 | 1.198242 | 0.001221494 | 21.70583 | 986.6288 | 0.000407165 |
| 0.030955 | 0.098159 | 0.815301 | 1.208008 | 0.001218708 | 22.067 | 1003.045 | 0.000406236 |
| 0.031413 | 0.097527 | -1.2477 | 1.217773 | 0.001236716 | 21.92493 | 996.5876 | 0.000412239 |
| 0.03144 | 0.09706 | 1.347168 | 1.227539 | 0.001237804 | 21.81996 | 991.8164 | 0.000412601 |
| 0.031748 | 0.098385 | 0.311643 | 1.237305 | 0.001249934 | 22.11775 | 1005.352 | 0.000416645 |
| 0.032054 | 0.098773 | 0.734743 | 1.24707 | 0.001261969 | 22.20516 | 1009.325 | 0.000420656 |
| 0.033881 | 0.100163 | -1.2178 | 1.256836 | 0.001333893 | 22.51762 | 1023.528 | 0.000444631 |
| 0.032026 | 0.099483 | 1.206845 | 1.266602 | 0.001260867 | 22.36467 | 1016.576 | 0.000420289 |
| 0.033369 | 0.100252 | 0.311719 | 1.276367 | 0.001313745 | 22.53765 | 1024.439 | 0.000437915 |
| 0.032286 | 0.100762 | 0.619802 | 1.286133 | 0.001271107 | 22.65223 | 1029.647 | 0.000423702 |
| 0.033923 | 0.103059 | 0.14695 | 1.295898 | 0.001335543 | 23.16857 | 1053.117 | 0.000445181 |
| 0.033054 | 0.103046 | 1.089096 | 1.305664 | 0.001301336 | 23.16564 | 1052.984 | 0.000433779 |
| 0.034025 | 0.101779 | 0.772254 | 1.31543 | 0.00133956 | 22.88072 | 1040.033 | 0.00044652 |